# Zhangfei Suppresses the Growth of Medulloblastoma Cells and Commits Them to Programmed Cell Death

A Thesis Submitted to the College of Graduate Studies and Research in Partial Fulfillment of the Requirements for the Masters of Science Degree in the Department of Veterinary Microbiology at the University of Saskatchewan, Saskatoon, Canada.

By
Timothy Wayne Bodnarchuk

Permission to Use

In presenting this thesis in partial fulfillment of the requirements for a Postgraduate degree from the University of Saskatchewan, I agree that the Libraries of this University may make it freely available for inspection. I further agree that permission for copying of this thesis, in any manner, in whole or part, for scholarly purposes may be granted by the professor or professors who supervised my thesis work or, in their absence, by Head of the Department or Dean of the College in which my work was done. It is understood that any copying or publication or use of my thesis or part thereof for financial gain shall not be allowed without my written permission. It is also understood that due recognition shall be given to me and to the University of Saskatchewan in any scholarly use which may be made of any material in my thesis.

Request for permission to copy or to make other use of material in this thesis in whole or part should be addressed to:

Head of the Department of Veterinary Microbiology
University of Saskatchewan
52 Campus Drive
Saskatoon, Saskatchewan S7N 5B4

**Abstract**

Medulloblastoma cells do not contain detectable amounts of the bZIP protein Zhangfei. However, previous work has shown that expression of this protein in cells of the ONS-76 line, derived from a human medulloblastoma, causes the cells to stop growing and develop processes that resemble neuritis (a characteristic of differentiated neurons). Zhangfei-expressing cells eventually die. My objective was to determine the molecular mechanisms by which Zhangfei influences ONS-76 cells. My strategy was to infect ONS-76 cells with adenovirus vectors expressing either Zhangfei or the control *E. coli* protein β-galactosidase (LacZ) and then to compare the following parameters in Zhangfei and LacZ-expressing cells: a) markers of apoptosis, autophagy and macropinocytosis (the three main pathways of cell death); b) transcripts for genes involved in neurogenesis and apoptosis; c) phosphorylation of peptide targets of selected cellular protein kinases; and d) active transcription factors. Zhangfei-expressing cells appeared to succumb to apoptosis as determined by the expression of phosphatidylserine on the cell surface and intensity of nuclear staining with the DNA dye Hoechst. Increased staining for autophagic vesicles and upregulated expression of autophagy response genes in these cells indicated that they were undergoing autophagy, possibly associated with apoptosis. My analysis of steady-state transcripts for genes involved in apoptosis and neurogenesis and functional protein kinases in Zhangfei-expressing cells indicated that the mitogen-activated protein kinase (MAPK) pathway was active in these cells. In addition, I found that the transcription factor Brn3a as well as factors implicated in differentiation were also active. These observations led me to hypothesize that Zhangfei enhances the expression of Brn3a, a known inducer of TrkA, the high-affinity receptor for nerve growth factor (NGF). TrkA then binds in an autocrine manner to NGF, triggering the MAPK pathway and leading to differentiation of ONS-76 cells into neuron and glia-like cells, eventually bringing about cell death by apoptosis and autophagy. I tested this hypothesis by showing that Zhangfei could enhance transcription from the isolated Brn3a promoter, that ONS-76 cells produce NGF as detected in a bioassay, and that antibodies against NGF and inhibitors of TrkA and selected components of the MAPK pathway could partially restore the growth of Zhangfei-expressing ONS-76 cells. My work supports previous work highlighting the importance of NGF-TrkA signaling in the outcome of medulloblastomas and shows how Zhangfei is able to trigger this pathway.

**Keywords:** Zhangfei, TrkA, MapK, medulloblastoma, Brn3a, apoptosis, autophagy, macropinocytosis.

**Acknowledgments**

Funding for this research and my stipend was provided in part by an NSERC discovery grant awarded to Dr. Vikram Misra, as well as a Departmental Devolved Scholarship. My sincerest thanks go to the University of Saskatchewan faculty and support staff, without whom this research would not be possible. We must always remember that scientific study is meaningless unless it can be explained simply and with purpose to those who fund our endeavors, the citizens of Canada.

I would like to thank Dr. Vikram Misra for his guidance, time, and molecular genius. Your love of science is an inspiration.

To Noreen, thank you for all of your help and conversation. We have shared many laughs, stories, … and laboratory reagents. I wish you and your family all the best.

Iran, I wish you much future success and happiness. You have one of the kindest hearts I have ever, or will ever meet. I have the honor of calling you my friend.

Thank you to all of WVCM friends and fellow graduate students. I'm sure that most of you would have gotten more work done if it wasn't for me. You are welcome. ;)

I dedicate this publication to my dearest family and friends: Mom, Dad, Brenda, Roy, Amy, and Stavros. Thank you.

**Table of Contents**

**List of Figures:**



**List of Tables:**

**List of Abbreviations:**

| | |
|---|---|
| ADORA2A | adenosine A2a receptor |
| ALK | anaplastic lymphoma receptor tyrosine kinase |
| AP-1 | complexes between c-Jun, c-Fos, ATF, and JDP |
| AP-2 | transcription factor AP-2 |
| Apaf-1 | apoptotic peptidase activating factor 1 |
| APBB1 | amyloid beta precursor binding protein 1 |
| APO3 | apoptosis inducing receptor 3 |
| AR | androgen receptor |
| ATF | activating transcription factor |
| ATG | autophagy related homolog |
| β-gal | beta galactosidase |
| bZIP | basic leucine zipper |
| BCL2 | B-cell CLL/lymphoma 2 |
| BMP15 | bone morphogenic protein 15 |
| BMP2 | bone morphogenic protein 2 |
| BMP8B | bone morphogenic protein 8 B |
| bp | base pair |
| BDNF | brain derived neurotrophic factor |
| Brn3a | brain specific homeobox/POU domain protein 3A |
| c-Fos | FBJ murine osteosarcoma viral oncogene homolog |
| c-Jun | Jun proto-oncogene |

| | |
|---|---|
| c-Myc | myelocytomatosis viral oncogene homolog |
| c-Src | v-src sarcoma viral oncogene homolog |
| cAMP | cyclic adenosine monophosphate |
| CASP | caspase family member |
| CAT | chloramphenicol acetyl transferase |
| CBF | CCAAT-box-binding transcription factor zeta |
| CCM2 | cerebral cavernous mal-formation-2 |
| CD40 | cell determinant 40 (recently renamed as: tumor necrosis factor receptor superfamily member 5) |
| CIDEA | cell death-inducing DFFA-like effector A |
| CRE | cAMP response element |
| CREBP | cAMP response element binding protein |
| D-MEM | Dulbecco's modified Eagle's medium |
| DISC | death-inducing signaling complex |
| DLG4 | disk large homolog 4 |
| DMSO | dimethylsulfoxide |
| DNA | deoxyribonucleic acid |
| DR3 | death receptor 3 |
| DUSP1 | dual specificity phosphatase 1 |
| EDTA | ethylenediaminetetraacetic acid |
| EGF | epidermal growth factor |
| Egr-1 | early growth response 1 |
| Elk-1 | ETS oncogene family member 1 |

| | |
|---|---|
| EPHA2 | ephrin type-A receptor 2 |
| ERK | extracellular signal-related kinase |
| FASL (APO-1 Ligand) | tumor necrosis factor superfamily member 6 ligand |
| FASR (APO-1) | tumor necrosis factor superfamily member 6 receptor |
| FAST-1 | forkhead box H1 |
| FBS | fetal bovine serum |
| FGF | fibroblast growth factor |
| FoxO | forkhead box 01 |
| GAP-43 | growth associated protein-43 |
| GAPDH | glyceraldehyde 3-phosphate dehydrogenase |
| GCP | granule cell precursors |
| GDNF | glial cell derived neurotrophic factor |
| GDP | guanosine diphosphate |
| GTP | guanosine triphosphate |
| HCF | host cellular factor |
| hpi | hours post-infection |
| HSV | herpes simplex virus |
| IAP | inhibitor of apoptosis |
| JDP | Jun dimerization partners |
| JNK | c-Jun N-terminal kinase, MAPK8 |
| IRF | interferon regulatory factor |
| LC3 | microtubule-associated protein 1 light chain |
| MAPK | mitogen activated protein kinase |

| | |
|---|---|
| MEF-2 | myelin expression factor 2 |
| MEK | mitogen-activated protein kinase kinase 1 |
| MHC | major histocompatibility complex |
| MOI | multiplicity of infection |
| mTOR | mammalian target of rapamycin |
| NF | neurofilament |
| NFATC2 | nuclear factor of activated T-cells, cytoplasmic 2 |
| NFκB | nuclear factor kappa B |
| NK | natural killer |
| NGF | nerve growth factor |
| NT3 | neurotrophins 3 |
| NT4 | neurotrophins 4 |
| P38 | mitogen-activated protein kinase 14 |
| p53 | tumor protein 53 |
| PBS | phosphate buffered saline |
| PCR | polymerase chain reaction |
| pfu | plaque forming unit |
| PI3K | phosphoinositide 3′-kinase |
| PKC | protein kinase C |
| PRKCA | protein kinase C alpha |
| PRKCB | protein kinase C beta |
| PTB | phosphotyrosine-binding domain |
| qRT-PCR | quantitative real-time polymerase chain reaction |

| | |
|---|---|
| Raf | murine leukemia viral oncogene homolog 1 |
| RAS | protein-specific guanine nucleotide-releasing factor 1 |
| RelA | nuclear factor NF-kappa-B p65 subunit |
| S100B | S100 calcium binding protein B |
| SATB | SATB homeobox 1 |
| SH2 | Src homology 2 domain |
| SHC | Src homology domain containing protein |
| SMAC/DIABLO | IAP-binding mitochondrial protein |
| SOS | son of sevenless homolog 1 |
| Sp-1 | transcription factor Sp1 |
| Src | Schmidt-Ruppin viral oncogene homolog |
| SRE | serum response element |
| Stat6 | signal transducer and activator of transcription 6 |
| TAK1 | nuclear receptor subfamily 2, group C, member 2 |
| TGFβ | transforming growth factor beta |
| TNFα | tumor necrosis factor alpha |
| TNFRSF9 | tumor necrosis factor receptor superfamily member 9 |
| TrkA | tropomyosin related kinase A |
| TrkB | tropomyosin related kinase B |
| TrkC | tropomyosin related kinase C |
| VP16 | virion protein 16 |
| WIP1 | wild-type p53-induced phosphatase 1 |
| ZF | Zhangfei (CREBZF) |

# Chapter 1: Introduction

## 1.1 Literature Review

The goal of the following literature review is to provide the reader with background information on medulloblastoma brain cancer, death pathways in neuronal tumors, neuronal differentiation, and the signaling pathways that mediate these processes. I will discuss these topics in the context of my hypothesis, in which I propose that transcriptional regulator protein Zhangfei activates what appears to be neuronal differentiation and programmed cell death in the medulloblastoma cell line ONS-76. I will begin by providing an introduction to medulloblastoma brain cancer, tropomyosin related kinase A (TrkA) signaling in neuronal cells, and Zhangfei. Following that, I will provide information on death signaling in neuronal cells by apoptosis, autophagy, and macropinocytosis, along with the signaling pathways that activate and control these processes. It should be noted that apoptosis and autophagy have been described as mechanisms of programmed cell death, while macropinocytosis, to date, has not. I will conclude the literature review with my rational, hypothesis, and objectives.

### 1.1.1 Introduction to Medulloblastomas

Medulloblastomas are invasive, rapidly growing brain cancers that generally arise in children. They comprise about 16% of all infant brain tumors, 40% of all cerebral tumors in children under the age of 20, and approximately 2.0% of all adult brain cancers

(26). Medulloblastomas are one of the few brain tumors that are able to spread via cerebrospinal fluid leading to metastasis to different locations within the brain and spinal cord. Current treatment for medulloblastomas involves excision of the tumor followed by radiation, chemotherapy, or both (reviewed in 26). While these treatments do improve survival, it is often at the cost of severe brain damage and loss of quality of life for long-term survivors. Additionally, despite treatment, one third of medulloblastomas remain incurable (41).

### 1.1.2 Development of Medulloblastomas

Some medulloblastomas are thought to arise from granule cell precursors (GCP) (12, 64). In normal development (during late embryogenesis and early childhood), GCP's are induced to divide and then migrate to the cerebral core. This process is mediated by the Sonic Hedgehog (148), and Notch signaling pathways (reviewed in 41). As the GCP's divide and migrate, the effects of the Sonic Hedgehog pathway are countered by factors such as fibroblast growth factor and the cells differentiate into mature granule cell neurons (37, 148). GCP's can also differentiate into astroglial cells due to the effects of bone morphogenic protein 2 (BMP2) (100). Cells of the medulloblastoma cell line ONS-76 reflect these bipotent characteristics and display properties of both glial and neuronal precursors (103, 135). This bipotency is exemplified by the ability of these cells to express major histocapatibility complex I (MHC-I) and MHC-II (a characteristic of glial cells); they also express neurofilament

protein and enolase 2, characteristic of neuronal cells. The ONS-76 cell line was created by Tamura *et al.* using a tumor removed from a two year old female in 1987 (135).

### 1.1.3 Tropomyosin Related Kinase A (TrkA)

Tropomyosin related kinase A (TrkA) belongs to a family of receptor tyrosine kinases that include TrkB and TrkC. These receptors exist in the plasma membrane of cells of neuronal origin and act to regulate neuronal survival, proliferation and plasticity. Ligands activating these receptors are: NGF (nerve growth factor), brain derived neurotrophic factor (BDNF), and neurotrophins 3 and 4 (NT3, NT4). Upon binding of ligand, these receptors dimerize and activate signaling pathways. The primary signaling pathway activated by TrkA is the MAPK (mitogen activated protein kinase) pathway (reviewed by Huang *et al.*, 54). A detailed diagram of the MAPK signaling pathway mediated by TrkA is available in Figure 1.1. TrkA is also known as the high-affinity NGF receptor, and as its name suggests, NGF is its primary ligand. TrkA is expressed at relatively low levels in the ONS-76 medulloblastoma cell line in comparison to mature, differentiated neurons (143). The expression of TrkA in neurons is influenced by transcription factor Brn3a in addition to other factors (141). For the sake of clarity, MAPK will be used to refer to the MAPK signaling pathway as a collective, while ERK1/2 (members of the pathway, also known as MAPK) will be referred to as ERK.

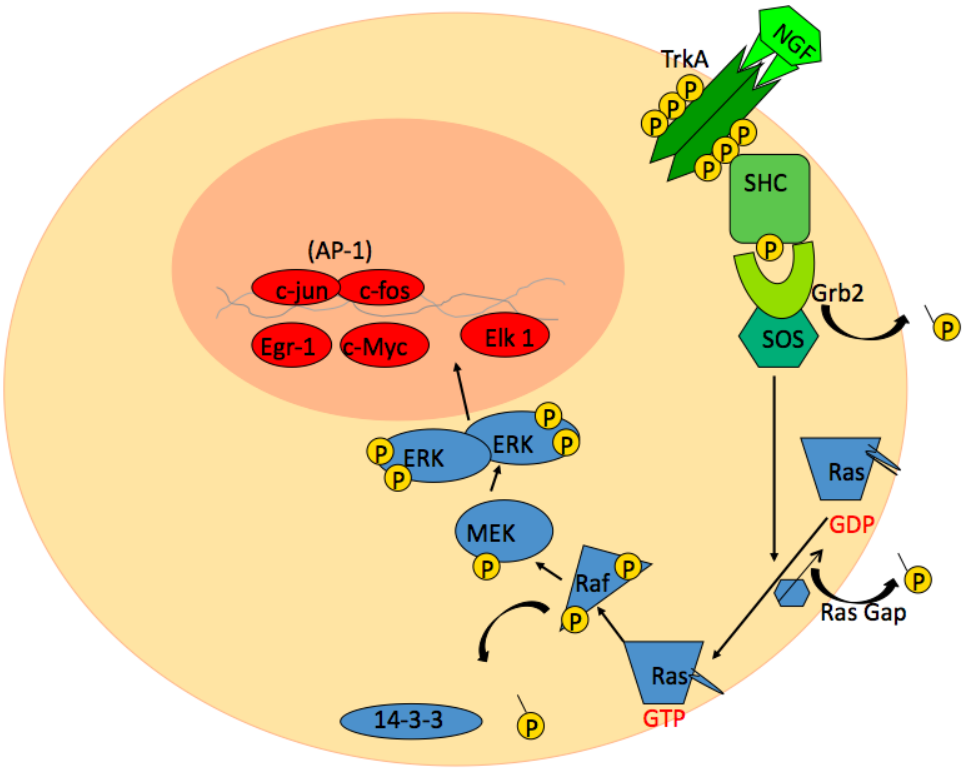


**Figure 1.1. MAPK Signaling.** When inactive in the plasma membrane of cells, TrkA exists as a monomer. Upon binding of ligand, nerve growth factor, the receptors dimerize and undergo auto-trans-phosphorylation in their kinase domain, followed by phosphorylation at the SHC binding domain. This event triggers the beginning steps of the MAPK kinase pathway. SHC is able to bind the phosphorylated receptor via its PTB phosphoprotein binding domain. Binding of SHC results in it's phosphorylation. Adaptor protein Grb2 binds phosphorylated SHC via its SH2 phosphoprotein-binding domain. Grb2 may bypass this step completely and bind the phosphorylated receptor. Grb2 is constitutively bound to another protein, SOS, via two SH3 protein-binding domains. SOS is a guanine nucleotide exchange factor, and acts as an activator for the next protein in the MAPK pathway, Ras. Ras is a monomeric G-protein with a prenylated C-terminus for association with the plasma membrane. Upon interaction with activated SOS, Ras releases its bounds GDP and exchanges it for a GTP. Activated Ras recruits, binds, and activates Raf by causing a dephosphorylation event. Inactive Raf is phosphorylated at regulatory sites and exists in the cytosol bound to the regulatory protein 14-3-3. Dephosphorylation of Raf results in loss of 14-3-3, then phosphorylation of Raf by other kinases including PKC (protein kinase C) and c-Src. Activated Raf is then able to phosphorylate MEK, which in turn phosphorylates ERK (also known as MAPK). MEK is a dual specificity kinase, meaning that it is capable of phosphorylating both tyrosine and threonine residues (which it does to ERK). Phosphorylated ERK dimerizes and is imported into the nucleus, where it is able to phosphorylate nuclear transcriptional elements and transcription factors (including: Elk-1, Egr-1, c-Myc, as well as c-Fos and c-Jun, or known together as AP-1) leading to their activation. Reviewed by Lodish *et al.* (75).

### 1.1.4 TrkA-Mediated Transcription

Trophic responses to TrkA signaling are mediated through the MAPK signaling cascade (62). The primary transcription factor targets of MAPK signaling include: c-Fos (FBJ murine osteosarcoma viral oncogene homolog), c-Jun (Jun proto-oncogene), Egr-1 (early growth response 1), Elk-1 (ETS oncogene family member 1), c-Myc (myelocytomatosis viral oncogene homolog), and AP-1. Transcription factor AP-1 refers to heterodimeric and homodimeric complexes between c-Jun, c-Fos, ATF (activating transcription factors), and JDP (Jun dimerization partners) families of transcription factors that bind to the AP-1 recognition site in DNA (127). AP-1 family members have been shown to both promote differentiation/survival as well as apoptosis in a very cell-specific and signal specific manner (4). AP-1 activation has been shown to play a role in neuronal differentiation of mouse bone marrow stromal cells (154). This differentiation is also ERK dependent. Feng *et al.* also found that AP-1 activity was required for neuronal differentiation (36). Egr-1 activity is upregulated in the developing brain (83), but has also been identified as a candidate to induce apoptosis in conjunction with c-Myc (8). It is clear that the transcription factors targeted by TrkA signaling play a complex and highly regulated role in cellular survival and death.

### 1.1.5 TrkA Retrograde Signaling

After prolonged activation of TrkA, the receptor is endocytosed. It continues to signal under what is called the "retrograde" pathway until the time when it fuses with a

degradative vesicle or is recycled (109). Retrograde TrkA signaling still requires MAPK pathway members to mediate its function. One notable MAPK family member shown to mediate retrograde signaling is ERK5. ERK5 has been shown to be active during retrograde signaling and phosphorylate target transcription factors including CREB and Mef2 (114, 147). A diagram of retrograde signaling can be viewed in Figure 1.2.

### 1.1.6 TrkA in Neuronal Survival, Differentiation and Death

TrkA has been studied for its role in cellular differentiation and promoting cellular survival. Neuronal differentiation involves exit from cell cycle and the growth of cellular projections known as neurites. Neurofilament helps to maintain the shape and rigidity of these neurites (57). Kimmelman *et al.* found that ectopic expression of RAS (Ras protein-specific guanine nucleotide-releasing factor 1; a member of the MAPK signaling pathway) in PC12 cells (pheochromocytoma of the rat adrenal medulla) was sufficient to induce differentiation (65). Differentiation was dependent on MAPK signaling activation and was detected by neurofilament production, growth-associated protein 43 (GAP-43) production, and neurite growth. Dimitropoulou *et al.* have shown the importance of MEK and ERK activation in the development of chick retinal neurons (30). MEK (mitogen-activated protein kinase kinase 1) and ERK (mitogen-activated protein kinase 1) are key members of the MAPK signaling pathway. To further complicate the role of TrkA signaling, these observations are often tissue specific.

While TrkA signaling is involved in neuronal differentiation and survival, it can also mediate the death of neuronal cells (49, 87, 95, 104). TrkA expression is increased

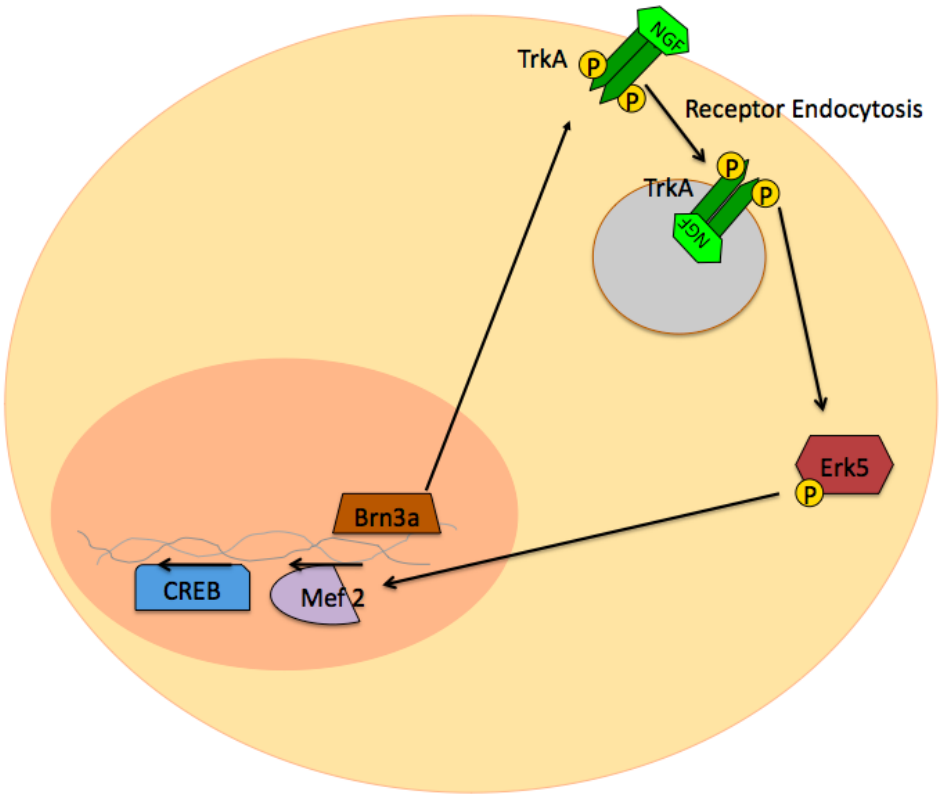


**Figure 1.2. TrkA Retrograde Signaling.** With prolonged stimulation, the TrkA receptor is endocytosed where it continues to signal, through ERK5. Transcription factors targeted by retrograde signaling include CREB and Mef2. Refer to text for further detail.

in segments of the cerebellum during differentiation, and correlates with a increased apoptotis (99). Expression of TrkA also correlates with lower grade neuroblastoma tumors (13, 96) and NGF treatment of medulloblastoma cells expressing TrkA induces the death of these cells (95). TrkA may also direct apoptosis in neuronal cells by induced cleavage of the p75 neurotrophin receptor (87). This cleavage results in the activation of the caspase cascade bringing about cell death by apoptosis (139). Cerebral cavernous mal-formation-2 (CCM2) has also been shown to mediate TrkA-induced apoptosis in medulloblastoma cells by directly binding to juxtamembrane region of this NGF receptor and linking its signaling to cell death pathways (49).

### 1.1.7 Zhangfei (CREBZF)

Ectopic expression of the protein Zhangfei (CREBZF) in ONS-76 medulloblastoma cells results in the transcript levels of TrkA increasing by more than ten fold, along with cessation of growth followed by what appears to be cellular differentiation and cell death (143). Zhangfei is expressed in mature neurons, but cannot be detected in neuronal tumors, including the cell line ONS-76 (1).

Zhangfei was originally identified as a partner for Host Cellular Factor, a co-activator of the herpes simplex virus (HSV) transactivator VP16 (77). It is a potent inhibitor of VP16 and HSV replication (1). Zhangfei is a basic leucine zipper (bZIP), meaning it has a basic domain, which in other bZIP proteins binds to elements in the promoters of responsive genes. bZIP proteins also have a leucine zipper domain used to interact with other bZIP proteins. The basic domain of Zhangfei lacks an asparagine

residue shown to be critical for promoter recognition in other bZIP proteins and, perhaps, as a consequence of this, Zhangfei does not bind known bZIP response elements (52, 77, 91). The inability of Zhangfei to bind known bZIP response elements as a homodimer is conserved in homologs of other vertebrates, including the Japanese puffer fish (22). While Zhangfei does not appear to activate transcription on its own, it may do so in association with other bZIP proteins. bZIP proteins form homodimeric and heterodimeric complexes (52, 77). Zhangfei is no different, although its homodimer has been described as relatively unstable, and unable to bind DNA, leading to the hypothesis that Zhangfei must form heterodimers in order to act as a transcriptional regulator (52, 77). One such Zhangfei binding partner is ATF4 (activating transcription factor 4, or CREB2). Zhangfei was shown to enhance binding of ATF4 to the CRE (cyclic-AMP response element) and increase its transcriptional activation in response to MEK1 (mitogen-activated protein kinase 1) signaling. Interestingly, MEK1 is a member of the MAPK signaling pathway, the primary signaling pathway of TrkA.

As mentioned previously, Zhangfei has been shown to upregulate the expression of TrkA in ONS-76 cells and induce their death (143). Many studies also link the expression of TrkA to cell death (see section 1.1.6). The following sections explore cellular death pathways and the molecular mechanisms by which they are regulated.

### 1.1.8 Death Pathways

An important characteristic of cancer cells is their uncontrolled division coupled with a resistance to cell death. Thus, when studying medulloblastoma tumor cells it

becomes important to understand the mechanisms of induced cell death, cessation of division, and differentiation. Three methods of programmed cell death appear in the literature: apoptosis, macropinocytosis, and autophagy (48, 72, 118).

### 1.1.9 Apoptosis

Apoptosis is a complex series of biochemical and morphological events that lead to cell death. The term apoptosis was first used by Kerr *et al.* in 1972, in which he described a distinct "mechanism of controlled cell deletion, which appears to play a complementary but opposite role to mitosis" (63). Work by Horvitz *et al.* in 1999 on the developing nematode *Caenorhabditis elegans* led to much of our current understanding on the role of apoptosis in developing organisms, the molecular and genetic means of apoptosis, and the evolutionary conservation of these pathways (53). Apoptosis is so well conserved in fact, there has been considerable documentation of this process occurring in plants (129, 144, 145). Apoptosis is also known to dominate the process of tadpole tail regression during *Xenopus* metamorphosis (121), shaping the middle ear (35, 115, 150), and in creating the spaces between our fingers and toes (156).

Apoptosis occurs as a natural and essential part of everyday physiology. It is required for the maintenance of cellular homeostasis, the development and preservation of the immune system, as a defense mechanism against infection and toxins, and in eliminating cells damaged following irradiation or chemical exposure. It has been estimated that a human adult loses 10 billion cells per day to apoptosis to allow for tissue homeostasis alone (113). Apoptosis is critical for the removal of autoreactive immune

cells, and furthermore, it is the mechanism by which natural killer and cytotoxic T-cells protect our bodies against infection, reviewed in (34). Irreversible damage to DNA by either irradiation or noxious chemicals may trigger apoptosis (98). This response is essential to prevent mutation, cancer, and to mediate effective cleanup of damaged cells (67, 76, 116).

### 1.1.10 Apoptosis and Cancer

The process of apoptosis becomes especially significant when studying cancer. Apoptosis, being a genetically coded process, may be affected by mutation. Mutations in apoptotic machinery or regulatory proteins may cause or contribute to disease, such as tumorigenesis (76, 136). A key characteristic of metastasis is the ability of a cancerous cell to survive in the absence of contact with other cells following its break from its tissue of origin, and invasion into other tissues. The work by Frisch *et al.* shows that disruption of epithelial cell-cell or cell-matrix interactions can lead to apoptosis (38). The process of apoptosis occurring following loss of contact to a substratum is termed “anoikis”. Aside from naturally induced apoptosis in cancerous cells, the majority of anti-cancer agents used today, such as chemotherapeutic agents and radiation, work by inducing apoptosis (119).

### 1.1.11 The Morphology of Apoptosis

Apoptosis is characterized by a set of morphological changes. Early changes when a cell first begins to undergo apoptosis include cell shrinkage and pyknosis (chromatin condensation) (63). This process is followed by budding of the plasma membrane, karyorrhexis (fragmentation of the nucleus), exposure of phosphatidylserine to the outer leaflet of the plasma membrane, degradation of chromosomal DNA, and cytoskeletal reorganization (46, 123). An important feature of apoptosis is that the plasma membrane maintains its integrity throughout this process, as to not leak any cellular contents or produce an inflammatory response. Phosphatidylserine along with other "eat me" signals facilitate engulfment of the apoptotic bodies (55).

Apoptosis is distinguishable from oncosis, cell death brought about in an unprogrammed manner. Oncosis, often misused as the term necrosis, and in contrast to apoptosis, is an energy independent process that usually affects a large number/area of cells at any one given time. Oncosis is usually due to direct disruption of the cell membrane or interruption of cellular nutrient supplies (82, 157). Other features of oncotic cell death include: cell swelling, loss of plasma membrane integrity, an inflammatory response, and swollen or ruptured mitochondria, reviewed in (32).

### 1.1.12 The Three Arms of Apoptosis

The molecular pathways involved in apoptosis are highly regulated and complex. There are three pathways known to be involved in apoptotic signaling: extrinsic, intrinsic,

and the perforin/granzyme pathway. All three pathways converge at a single point, caspase 3 activation. Caspase 3 activation is the first step in the execution stage of apoptosis. Figure 1.3 outlines these three death pathways.

### 1.1.13 Extrinsic Pathway

Activation of extrinsic apoptotic signaling involves interaction between death receptors and their cognate ligand. Death receptors belong to the tumor necrosis family of receptors. Examples of such receptor-ligand death receptors include: TNFα/TNFR1 (tumor necrosis factor alpha/tumor necrosis factor receptor 1), FASL/FASR (tumor necrosis factor superfamily member 6 and receptor), and APO3/DR3 (apoptosis inducing receptor 3/death receptor 3) (5, 125). Receptor signaling subsequently leads to DISC (death-inducing signaling complex) formation. DISC refers to an adaptor protein-initiator caspase complex that is involved in the activation of caspase 8, which in turn, activates caspase 3 (108). Caspase 3 activation is critical is the execution stage of apoptosis, bringing about the phenotypic characteristics of apoptosis described above (110). Caspases exist as inactive proenzymes (procaspases) within the cell. Activation of a caspase often allows for the activation of the following caspase in the sequence by proteolytic cleavage (50). This sequence of caspase activation is referred to as a cascade, hence the term "caspase cascade". Although caspase 3 appears to be the convergence point of all three apoptotic pathways, caspase 3 independent apoptosis has been documented. Didenko *et al.* found that apoptosis in rat brain ischemia cases did not rely on caspase 3 upregulation or activity (29). Brown *et al.* report that the cell line WEHI-

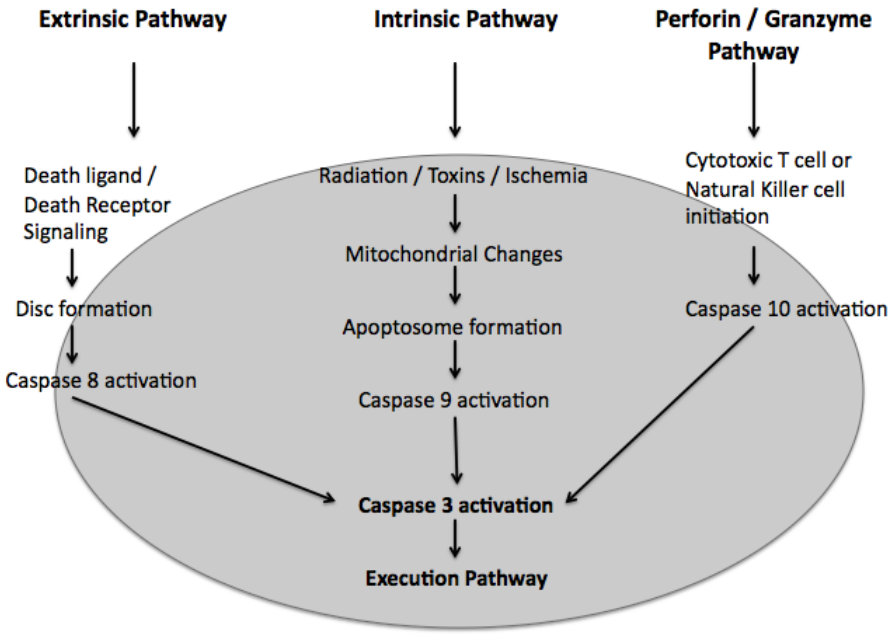


**Figure 1.3. The Three Arms of Apoptosis Induction.** Apoptosis may be achieved utilizing the extrinsic, intrinsic, or perforin/granzyme pathways. All three pathways converge at caspase 3 activation, often the first step in the execution pathway leading to cell death (figure adapted from Elmore *et al.*, 32).

231 undergoes caspase 3 independent apoptosis upon the addition of transforming growth factor beta (TGFβ) (14). Tumor necrosis factor alpha (TNFα) has also been reported to induce caspase 3 independent cell death in neuroblastoma cells (3).

### 1.1.14 Intrinsic Pathway

Activation of the intrinsic pathway of apoptosis may be brought about by numerous stimuli that signal a mitochondrial response. Such factors include: loss of growth factor stimulation, hypoxia, toxins, radiation, free radicals, and infection by a pathogen (reviewed in 32). Sufficient stimulation by any, or all, of these factors results in a loss of mitochondrial membrane potential and the leakage of pro-death substrates into the cell, such as Smac/DIABLO and cytochrome C (122). Smac/DIABLO works to promote apoptosis by inhibiting IAP's (inhibitors of apoptosis). Cytochrome C forms a complex with Apaf-1 (apoptotic peptidase activating factor 1) and procaspase 9 to form the "apoptosome." This results in the activation of procaspase 9. The apoptosome is then able to activate caspase 3 and initiate the process of apoptosis (20).

### 1.1.15 Perforin/Granzyme Pathway

The perforin/granzyme pathway of apoptosis is used by cytotoxic T-cells and natural killer T-cells to kill detectable tumor cells, or cells infected by pathogens. This mechanism involves the insertion of pore-forming molecules (perforin) into the target

cells plasma membrane. Following this, granules are released that travel through these pores into the target cell. One of these granules, granzyme B, is able to activate caspase 10, which in turn, activates caspase 3 to bring about death signaling. It should be noted that cytotoxic T-cells and natural killer cells also utilize the extrinsic apoptosis pathway by FASL/FASR signaling (15). The perforin/granzyme pathway is reviewed by Trapani *et al.* (137).

### 1.1.16 p53 and Apoptosis

Tumor protein 53 (p53) is one of the most highly recognized and studied tumor suppressor genes. TrkA has been shown to induce the expression of p53 in neuroblastoma cells, resulting in apoptosis (69). Work on NGF-mediated differentiation of PC12 cells has indicated a possible role for p53 in regulating TrkA levels (158). It was also found that phosphorylation of p53 on serine residues 6 and 9 may be required for proper p53-induced cessation of cellular division, and that phosphorylation of these residues was MAPK signaling dependent (25). Active and stable p53 is able to act as a transcription factor that has roles in regulating cell cycle, apoptosis, and differentiation (39). Although p53 appears to be the most commonly mutated gene in human cancers, medulloblastomas rarely contain mutated p53 sequences (18). Castellino *et al.* suggests that overexpression of WIP1 (an antagonist to p53-mediated apoptosis) may play a role in the tumorgenicity of medulloblastomas (18).

### 1.1.17 Introduction to Autophagy

Autophagy is the process by which a cell uses degradative lysosomes to degrade or recycle organelles and proteins. This process occurs naturally and regularly and is characterized by the formation of double membrane vesicles that enclose cellular constituents and fuse with lysosomes (68). Autophagy was first characterized as a response to cellular starvation. With further insight, it also appears to have a role in neurological disorders, cancer, organelle clearance and programmed cell death, notably in neurons (68, 84). The process of autophagy may be broken down into several sequential steps: induction, sequestration, degradation, and recycling of degraded constituents.

### 1.1.18 Autophagy as a Mechanism of Programmed Cell Death

Once thought to be only a pathway promoting cellular survival in times of nutrient starvation and in the recycling of dated cellular machinery, there is mounting evidence for autophagy as a mechanism of programmed cell death. In 1990 Clarke *et al.* devised a method of classification for programmed cell death, defining apoptosis as type 1 cell death, and autophagy as type 2 cell death based on the previous work of Scheichel *et al.* in 1973 (21, 126). Hansen *et al.* have discovered a novel pathway in which nerve growth factor stimulation of TrkA-transfected glioblastoma cells results in cell death by overactivation of autophagy (48). Confirmation of autophagy was performed by staining of acidic vacuoles with acridine orange, LC3-II production, and electron microscope photographs of cells containing many, large autophagic vacuoles. Bergmann *et al.* found

that autophagy was involved in *Drosophila melanogaster* development in a programmed manner (7). Xue *et al.* offer more support to the existence of autophagy as a death mechanism by showing that HELA, CHO, and cervical neurons treated with a death-inducing factor and an inhibitor of apoptosis are committed to cell death by autophagy (153). In contrast to cell death by apoptosis, autophagic cell death presents with only partial chromatin condensation, no DNA laddering, and nuclear fragmentation only at late stages. Plasma membrane budding may occur in both cases (reviewed in 44).

### 1.1.19 Autophagy and Cancer

The literature seems to be split on the role of autophagy in tumor biology. Some authors provide opinions suggesting that autophagy promotes tumor survival, while others suggest the opposite. Boya *et al.* and Lum *et al.* performed experiments limiting nutrients to tumor cells thereby increasing the rate of autophagy, and prolonging cellular survival (10, 79). In the hypoxic, nutrient-deprived environment of a tumor, this logic dictates that autophagy may provide a pro-tumor survival mechanism. In contrast to this idea, Beclin 1, an autophagy response gene, has been shown to act as a tumor suppressor gene in mice (111, 155). Also, the very idea that autophagy has been proposed as programmed cell death type 2, seems to contradict the idea that it would promote the survival of tumor cells. What is clear is that much more research into the role of autophagy in cancer is required.

### 1.1.20 Induction of Autophagy

Like apoptosis, the process of autophagy appears to be highly conserved, with detection in plants and yeast as well as animals (93, 134). Autophagy is generally upregulated in times of nutrient starvation. It has been suggested that autophagy is regulated, at least in part by the endocrine system, notably by insulin and glucagon *in-vivo* (92, 94). *In-vitro* studies utilize serum and/or amino acid starvation to activate autophagy. Much of hormone/growth factor/nutrient availability is thought to feed into mTOR (mammalian target of rapamycin) signaling (42, 45). TOR is thought to be a key regulator of autophagic induction, although how TOR actually detects these levels remains controversial (reviewed by Jung *et al.*, 58).

### 1.1.21 Autophagosome Formation and Sequestration

The process of autophagy begins with a phagophore (isolation membrane) surrounding the organelle or protein complex to be degraded. After total sequestration has occurred, the resulting structure is known as an autophagosome. Preliminary work and discovery of autophagic response genes was performed in yeast. 31 autophagy related (Atg) genes have been discovered to date, and are reviewed in detail (66, 131). Hallmarks of the autophagic process include cleavage of LC3 I (microtubule-associated protein 1 light chain 3 - 1) to LC3 II (microtubule-associated protein 1 light chain 2 - 2) for incorporation into the autophagic membrane, and upregulation of Beclin 1 (17, 60). The process of autophagy is outlined in Figure 1.4, in terms of autophagy response genes.

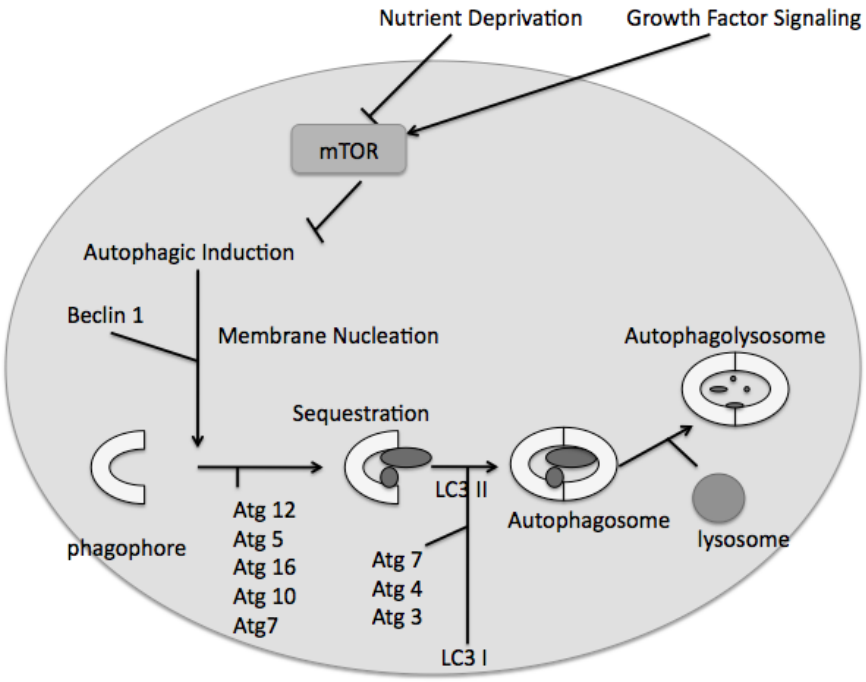


**Figure 1.4. A Brief Overview of Autophagy.** The above figure outlines the process of autophagy in terms of autophagy response genes. Beclin 1 is the mammalian homolog of ATG6, and LC3 is the mammalian homolog of ATG8. Refer to sections 1.1.20 - 1.1.22 for further detail.

### 1.1.22 The Autophagosome and the Autophagolysosome

After completion of the autophagosome, the compartment will fuse with lysosomes (or vacuoles in the case of plants and yeast). The contents of the autophagosome are degraded, along with the inner membrane of this double membrane structure and the structure is now referred to as a mature autophagolysosome (92). Larger molecules are broken down into their constituents to be recycled by the cell.

### 1.1.23 MAPK and JNK Signaling in Autophagy

MAPK signaling has been shown to inhibit the process of autophagy (24). In fact, MAPK signaling has been shown to activate mTOR, resulting in the inhibition of the autophagic induction process. Conversely, inhibition of mTOR has been shown to upregulate MAPK signaling (2). Wang *et al.* have shown that both depletion of ERK or inhibition of MEK leads to the inhibition of autophagy, suggesting a necessary role for MAPK signaling in inducing autophagy (146). These results may reinforce the importance of tissue specificity in cell signaling, a negative feedback loop, or perhaps a need for further exploration on the role of MAPK signaling in the induction of autophagy.

In contrast to the "grey area" of MAPK signaling in autophagy, the literature appears to be quite clear on the role of JNK signaling in autophagy. Zhang *et al.* found that Fas (tumor necrosis factor receptor superfamily member 6)-mediated autophagy is dependent on JNK signaling and that autophagy is inhibited with the use of a JNK

inhibitor (SP600125) (159). JNK was also found to be essential for the maintenance and survival of neurons by regulating FoxO (forkhead box 01)-dependent autophagy (152). Aside from its role in autophagy, JNK is also known to play a major role in the regulation of apoptosis, reviewed by Kanda *et al.* (61).

### 1.1.24 Introduction to Macropinocytosis

Macropinocytosis is a form of cellular endocytosis in which the cell takes up bulk amounts of extracellular fluids and dissolved solutes. Macropinocytosis has been the target of study for dendritic cell class II MHC restricted antigen uptake, apoptotic body uptake, as an entry mechanism for some viruses, and as a mechanism of cell death (33, 51, 89, 133). Macropinosomes differ from autophagosomes due to the fact that they are single membrane, rather than double membrane structures. The characteristics of apoptosis, autophagy and macropinocytosis are compared and contrasted in Table 1.5.

### 1.1.25 Mechanism of Macropinocytosis

The intake machinery required for macropinocytosis is described as a singular cellular lamellipodium that facilitates ruffling or folding of the plasma membrane (33, 133). These ruffles contain "cup shaped invaginations" (132). The fold seals in on itself, forming a vacuole known as a macropinosome. Macropinocytosis is easily distinguishable from micropinocytosis, which utilizes clatherin-coated, and small uncoated vesicles to take in relatively small amounts of substrate, usually in a selective

**Table 1.5. A Comparison Between Apoptosis, Autophagy, and Macropinocytosis.**

| Process | Apoptosis | Autophagy | Macropinocytosis | Oncosis |
|---|---|---|---|---|
| Cell Shrinkage (63) | x | | | |
| Pyknosis (63, 82) | x | | | x |
| Plasma Membrane Blebbing (32) | x | | | |
| Karyorrhexis (32, 82) | x | | | x |
| Cell Swelling (82) | | | | x |
| Karyolysis (82) | | | | x |
| Distension of Endoplasmic Reticulum (82) | | | | x |
| ATP and Caspase Depletion (157) | x | | | x |
| Cytoplasmic Vacuole Formation (140, 157) | | | | x |
| Swollen or Condensed Mitochondria (140, 157) | | | | x |
| Plasma Membrane Loss of Integrity (140, 157) | | | | x |
| Caspase Cascade Activation (23, 86, 102) | x | x | x | |
| DNA Fragmentation (9,102, 140) | x | | x | |
| Phosphatidylserine Exposed to Plasma Membrane Outer Leaflet (11) | x | | | |
| Cytochrome C, Smac/DIABLO Release from Mitochondria (122) | x | | | |
| Beclin 1 (ATG6) Upregulation (72) | | x | | |
| ATG5, ATG9 Upregulation (72) | | x | | |
| LC3 Cleavage/Acidic LC3-II Positive Double Membrane Vacuole Accumulation (72, 102) | | x | | |
| Incorporation of Organelles in Vacuoles (86) | | x | | |
| Single Membrane Vacuole Accumulation (102) | | | x | |

manner. Macropinocytosis on the other hand, takes in large amounts of extracellular fluid and solute macromolecules in a more or less unselective manner (133).

### 1.1.26 Macropinocytosis as a Death Pathway

Recently, macropinocytosis has been proposed as a possible mechanism of cell death. Li *et al.* have reported that NGF stimulation of DAOY strain medulloblastoma cells transfected to express TrkA results in cell death by hyperstimulation of macropinocytosis (72). Confirmation of macropinocytosis involved uptake of monodansyl cadaverin (MDC) into single membrane vacuoles, LC3-II production, and cell death independent of key members in autophagy and apoptosis pathways.

## 1.2 Rational, Hypothesis and Objectives

Previous results show that expression of Zhangfei in ONS-76 cells results in the growth of neurite-like projections followed by cell death (143). Zhangfei has also been shown to increase the expression of TrkA (143). The TrkA pathway has been shown to lead to neuronal cell death as well as differentiation (48, 72, 95, 104, 118). My hypothesis was that Zhangfei upregulates the expression of the high-affinity nerve growth factor, TrkA, resulting in the activation of signaling pathways that bring about possible differentiation followed by cell death.

My objective was to determine the molecular pathway(s) by which Zhangfei induces differentiation and/or cell death in ONS-76 medulloblastoma cells, and to

determine the type of cell death being activated. A photographic timeline of ONS-76 cells expressing Zhangfei or control protein, β-galactosidase, was performed to visibly show the phenotype of Zhangfei-expressing cells. A WST-1 proliferation and viability assay was used assess the viability of cells expressing Zhangfei. By using a combination of quantitative real-time polymerase chain reaction (qRT-PCR) arrays for detecting up-regulated gene transcripts, kinome arrays for identifying active protein kinases, and transcription factor analysis, potential pathways activated in Zhangfei-expressing ONS-76 cells were identified. Chemical inhibitors of kinases were used to elucidate and confirm the suspected signaling pathways. Next, a combination of fluorescent microscopy and flow cytometry guided the analysis of cellular death pathways, apoptosis, autophagy, and macropinocytosis.

The results suggest that Zhangfei acts by increasing the expression of Brn3a, a known regulator of TrkA transcription. TrkA activation by autocrine nerve growth factor stimulation could bring about downstream signaling that ultimately leads to cellular differentiation and death.

## Chapter 2: Materials and Methods

### 2.1 Cell Culture

The human medulloblastoma cell line ONS-76, (135), was obtained from Michael Taylor (University of Toronto, Canada). These cells were growth in Dulbecco's Modified Eagle Medium (D-MEM, Invitrogen, Carlsbad, CA, USA) high glucose with 10% fetal bovine serum (FBS, Invitrogen) and 1% penicillin–streptomycin (Invitrogen). This combination will be referred to as "complete media." Cells were cultured in a $CO_2$ incubator set at 37$^{o}$C and 5% $CO_2$ in 75cm$^2$ Falcon culture flasks or 6-well plates (BD Falcon, Mississauga, ON, Canada). The cell cultures were diluted 1/5 every three days. ONS-76 is an adherent cell line, as such, 0.05% Trypsin-EDTA (Invitrogen) was used to remove cells from the culture flasks and wells (3ml per culture flask, 250 µl per well in a 6-well plate).

D17 cells, obtained from American Type Culture Collection (ATCC), were grown in Alpha medium (Invitrogen) containing 10% FBS.

PC12 cells (provided by D. D. Mousseau, University of Saskatchewan) were grown in RPMI 1640 supplemented with 10% heat-treated horse serum, 5% fetal bovine serum, and 1% penicillin–streptomycin. Cells were grown on plates coated with collagen as follows: six-well plates were incubated at room temperature for 1 h with 2 ml of a 0.02 N acetic acid solution containing 50 µg/ml rat tail collagen (VWR). Plates were then rinsed with sterile PBS and used immediately. All components ordered from Invitrogen unless otherwise stated.

## 2.2 Adenovirus Vectors Expressing Zhangfei and β-galactosidase (LacZ)

These adenovirus vectors were constructed, grown, and purified using the Adeno-X Expression System (Clontech, Mountain View, California, USA). They were created previously in our laboratory (following the protocol outlined in 91). ONS-76 cells were infected with Adeno-Zhangfei (expressing human Zhangfei), Adeno-LacZ (expressing *E. coli* β-galactosidase) or mock-infected. Infection occurred by replacing the complete Dulbecco media from cells plated 24 hours previously, with 250 µl of OptiMEM (Invitrogen) diluted virus at a multiplicity of infection (MOI) of 100 plaque forming units (pfu) per cell. Cells were incubated at 37$^{o}$C in the $CO_2$ incubator for one hour, with rocking every 15 minutes. After the hour, 2 ml of complete Dulbecco's media was added.

## 2.3 WST-1 Cell Proliferation and Viability Assay

ONS-76 cells were plated in 96-well flat bottom Falcon plates at a concentration of $1x10^5$ cells per ml (100 µl per well) for a total of $1x10^4$ cells per well. Four hours later the media was removed, cells were rinsed with 100 µl of phosphate buffered saline (PBS) and then infected with either Adeno-Zhangfei or Adeno-LacZ (25 µl per well, MOI of 100 pfu/ml). After infection, 175 µl of fresh complete media was added to the wells. This media contained chemical inhibitors, if required (see Table 2.1 for concentrations). Plates were returned to the $CO_2$ incubator for 48 hours. 48 hours post-infection (hpi), 20

**Table 2.1. Chemical Inhibitors, Concentrations and Scientific Names.**

| Inhibitor | Concentration Used |
|---|---|
| JNK inhibitor SP600125 | 25 μM |
| p53 inhibitor (Pifithrin α) | 25 μM |
| MEK inhibitor PD98059 | 50 μM |
| CK1 inhibitor D4776 | 40 μM |
| TrkA inhibitor | 25 μM |
| ERK activation inhibitor II | 25 μM |
| Apoptosis inhibitor M50054 | 420 μM |

---

μl per well of WST-1 reagent (Clontech) was added. Cells were returned to the incubator for 1 hour before absorbance was measured at 450 nm (reference wavelength 650 nm) on a Molecular Devices, Vmax microplate reader. This colorimetric assay is based on the cleavage of the WST-1 reagent to a dye (detectable at 450 nm). Cleavage is accomplished by the mitochondrial enzyme succinate-tetrazolium reductase in metabolically active cells. The absorbance measured is directly related to the number of viable cells. All cell treatments were plated in triplicate. All chemical inhibitors were purchased from EMD Biosciences, VWR distributor, Mississauga, Ontario, Canada).

Rabbit anti-TrkA (Biovision, Mountain View, CA, USA) was used at a concentration of 1:500. Goat anti-NGF (nerve growth factor) and NGF were purchased from Cedarlane (Burlington, Ontario, Canada). Anti-NGF was used at a dilution of 1:100. This dilution was optimized to neutralize the effects of NGF at a concentration of 50 ng/ml.

### 2.4 mRNA Purification and cDNA Synthesis

An RNeasy Plus Mini Kit from Qiagen (Mississauga, ON, Canada) was used to purify mRNA from the ONS-76 cells. To ensure high quality RNA for qRT-PCR array analysis, samples were analyzed by electrophoresis on an Agilent 2100 Series Bioanalyzer, Eukaryotic Total RNA Nano series II, version 2.0. cDNA synthesis was performed on the extracted mRNA using the Quantitect Reverse Transcription Kit, also from Qiagen. 1 µg of template RNA at a time was converted to cDNA.

### 2.5 qRT-PCR Arrays and PCR Confirmation

Apoptosis and neurogenesis qRT-PCR arrays were purchased from SABiosciences (Frederick, MD, USA; array numbers PAHS-012 and PAHS-404, respectively). The arrays contain primers for 84 gene transcripts involved in a either apoptosis or neurogenesis. They also contain controls for genomic DNA contamination and reverse transcriptase efficiency. The results from triplicate experiments were analyzed by using an SABiosciences online resource called $RT^2$ profiler. Confirmation of qRT-PCR array results involved the development of primers. The primers were

designed using human mRNA gene sequences found on the NCBI human genome website (http://www.ncbi.nlm.nih.gov/projects/genome/guide/human/). Sequences were copied and pasted into a website tool called Primer3 (http://frodo.wi.mit.edu/primer3/). Primer3 picks potential primers based on the input selection criteria chosen. The criteria specified a product size between 180-300 base pairs, and a primer size between 18-23 base pairs. After designing, primers were purchased from Integrated DNA Technologies (IDT). Primers for ATG5 and ATG7 were designed by Wu et. al (151), and primers for ATG6 and BCL2 were designed by Lian *et al.* (74). qRT-PCR primer sequences for TrkA, Brn3a, and normalizer GAPDH are listed in the supplementary table S6 (143). Agilent Technologies' Brilliant II SYBR Green QPCR Master Mix Kit (catalog number 600828) was used to perform the qRT-PCR confirmation (in triplicate, also repeated 3 times. The PCR thermo-cycler used was a Stratagene Mx3005P model. Cycle details are as follows and based on manufacturers suggestions: segment 1 had 1cycle, 10:00 minutes at 95$^{o}$C; segment 2 had 40 cycles, the first at 95$^{o}$C for 30 seconds, the second at 55$^{o}$C for 1 minute, and the third at 72$^{o}$C for 1 minute; segment 3 had one cycle of 95$^{o}$C for one minute, 55$^{o}$C for 30 seconds and 95$^{o}$C for 30 seconds.

**2.6 Kinome Analysis**

ONS-76 cells were plated in sixteen, 250 ml 75 cm$^2$ Falcon culture flasks at a concentration of 2.5x10$^6$ cells per flask. The cells were allowed to adhere and recover overnight. Twelve hours later, the cells were washed in 5 ml OptiMEM, then infected with either 2 ml diluted Adeno-Zhangfei or Adeno-LacZ at an MOI of 100 pfu/ml, or

mock infected. The cells were then incubated at 37°C in the $CO_2$ incubator for one hour, with rocking every 15 minutes. After the hour, 10 ml of complete Dulbecco's media (D-MEM) was added. At the time of harvest (48 hours post-infection) the supernatants were collected and centrifuged (10 minutes at 500 x g) to collect all cells that had lost adherence to the flask, and added to the remaining cells that were collected by trypsinization (with 2 ml of trypsin for 10 minutes) in the $CO_2$ incubator. The cells from each group (Adeno-LacZ and Adeno-Zhangfei) were then individually pooled and centrifuged for 10 minutes at 500 x g. Supernatants were discarded and cell pellets were resuspended in 200 µl PBS. Cells were collected, pelleted and lysed by addition of 100 µl lysis buffer (20 mM Tris-HCL pH 7.5, 150 mM NaCl, 1 mM EDTA, 1 mM EGTA, 1% Triton, 2.5 mM sodium pyrophosphate, 1 mM $Na_3VO_4$, 1 mM NaF, 1 µg/ml leupeptin, 1 g/ml aprotinin, 1 mM PMSF), all products from Sigma-Aldrich, Ontario, Canada unless indicated. Cells were lysed on ice for 10 minutes and the cell debris was pelleted in a microcentrifuge for 10 minutes at 4 ºC. A 70 µl aliquot of the resulting supernatant was mixed with 10 µl of activation mix (50% Glycerol, 500 µM ATP (New England Biolabs, Pickering, Ontario, Canada), 60 mM $MgCl_2$, 0.05% v/v Brij-35, 0.25 mg/ml BSA), incubated on the array for 2 hours at 37 ºC. Arrays were then washed with PBS containing 1% Triton. Slides were submerged in phospho-specific fluorescent ProQ Diamond Phosphoprotein Stain (Invitrogen) with agitation for 1 hour. Arrays were then washed three times in destain containing 20% acetonitrile (EMD Biosciences, VWR distributor, Mississauga, ON) and 50 mM sodium acetate (Sigma-Aldrich) at pH 4.0 for 10 minutes. A final wash was done with distilled deionized $H_2O$. Arrays were air-dried for 20 minutes then centrifuged at 300 x g for 2 minutes to remove any remaining

moisture from the array. Arrays were analyzed using a GenePix Professional 4200A microarray scanner (MDS Analytical Technologies, Toronto, Ontario, Canada) at 532-560 nm with a 580 nm filter to detect dye fluorescence. Images were collected using the GenePix 6.0 software (MDS) and the spot intensity signal collected as the mean of pixel intensity using local feature background intensity background calculation with the default scanner saturation level.

The dataset contains the signal intensities associated with 300 peptides per array. ONS-76 cell groups (Zhangfei or LacZ-expressing) were collected in triplicate. For each treatment, there were three intra-array replicates.

The spot intensity of each peptide was calculated by subtracting background intensity from foreground intensity. The resulting data were transformed using a variance stabilization (VSN) model. The transformation brings all the data onto the same scale while alleviating variance-mean-dependence. In addition, for each of the 300 peptides in a single treatment, the average was taken over the three transformed replicate intensities. Note that the averaging was only applied in the subsequent clustering analysis not in the statistical inferences. Finally, the intensities induced by the treatments were adjusted by subtracting the intensities of the biological control (LacZ-expressing).

**2.7 Transcription Factor Profiling Array**

A transcription factor profiling array (Signosis BioSignal Capture, Sunnyvale, CA, USA) was used to determine which transcription factors were active in Adeno-Zhangfei-infected cells, relative to Adeno-LacZ-infected cells. This array measures the

ability of transcription factors to bind known DNA target sequences in the form of biotin labeled probes. The probes are then separated from unbound probes and the transcription factors, then hybridized to complementary DNA sequences in a 96-well plate. Results are produced by utilizing horse radish peroxidase conjugated streptavidin). Cells were plated at 2 x $10^6$ cells per well of a 6-well plate and infected at an MOI of 100 pfu/ml. Before the profiling array could be performed, the nuclear extracts from the ONS-76 cells were extracted with the use of the Signosis Nuclear Extraction Kit (Signosis). Protocols from kits were followed according to the manufacturers specifications.

### 2.8 Flow Cytometry and Fluorescent Microscopy

Flow cytometry and fluorescent microscopy were performed to evaluate cellular death pathways both quantitatively and qualitatively. Autophagy was detected by a Cyto-ID autophagy detection kit (ENZO life sciences, Plymouth Meeting, PA, USA). Instructions for flow cytometry and fluorescent microscopy were followed as per manufacturers recommendations. Detection of apoptosis by flow cytometry was performed with the use of an Annexin V staining kit (Calbiochem, VWR distributor Mississauga, Ontario, Canada). Fluorescent microscopy was performed with the use of a dual stain apoptosis detection kit (Piscataway, NJ, USA). Instructions for flow cytometry and fluorescent microscopy were followed as per manufacturers recommendations. Flow cytometry was performed using a Coulter EPICS XL flow cytometer.

Macropinocytotic vesicles were detected by fluorescent microscopy. ONS-76 and D17 cells (Manassas, VA, USA) were plated at 2x$10^5$ cells per well in 6-well Falcon

plates, each containing an 18mm, 1-ounce micro cover slip (VWR). Control cells were infected with Adeno-LacZ, treated cells received Adeno-Zhangfei, both at an MOI of 100 pfu/ml. 24 hours later, the media was replaced with fresh media containing Alexa 488-dextran (Invitrogen) at a concentration of 25 μg/ml. 24 hours later, the media was removed, 50 μl of it being replaced over the glass cover slips containing 10 nM of Lysotracker red (Invitrogen). The cells were incubated for 10 minutes in the $CO_2$ incubator. Next, the cells were washed 2 times with 100 μl of PBS. Coverslips were inverted onto glass slides and sealed with clear nail polish. Cells were examined immediately by fluorescent microscopy (Zeiss Axiovert, fitted with UV optics and CCD camera. Images were captured and analyzed using Northern Eclipse software (Mississagua, Ontario, Canada).

**2.9 PC12 Cell NGF Sensitivity Assay**

PC12 cells grow neurites in the presence of NGF. This assay was used to measure the approximate amount of NGF produced by ONS-76 cells (control, and Zhangfei-expressing). 24 hours after plating, the cells were treated with NGF (Cedarlane), goat anti-NGF (Cedarlane), NGF + anti-NGF, supernatant/cell lysate from ONS-76 cells expressing Zhangfei (250 μl), supernatant/cell lysate from ONS-76 cells expressing β-galactosidase (250 μl), or had the media replaced with fresh media and left as a control group. Supernatant and cell lysate from ONS-76 cells was collected at 48 hpi using cell scrapers (BD Falcon) to lift adherent cells from the plate bottoms. Next, the cell mixture was sonicated (Sonics and Materials, Danbury, CT, USA) for 5 seconds and

freeze-thawed 3 times to ensure all cells were lysed. Next, the cell debris was removed by centrifugation at 600 x g for 5 minutes to remove large chunks of cellular debris. Supernatants were collected and stored at -80$^{o}$C until use. PC12 cells with and without neurites were counted by phase contrast microscope using a 25x objective, 72 hours after treatment.

**2.10 CAT Assay and Brn3a Promoter Plasmid Design**

A 2047 base pair region upstream of the Brn3a gene (containing the promoter region) was amplified using PCR from ONS-76 cellular genomic DNA. The upstream primer (5′ GGTACCTAAAGACCAGCGCTTCCTTG 3′) contained Kpn1 restriction enzyme recognition site at its 5′ end. The downstream primer (5′ CTCGAGGACGGGA TGCACTCCTCTAAC 3′) contains a Xho1 restriction enzyme recognition site on its 5′ end. Restriction sites were used to facilitate cloning. The amplified 2047 base pair fragment was cloned using a TOPO cloning kit (Invitrogen). Next, the fragment was transferred to pCAT3basic (Clontech) pCAT3basic is a chloramphenicol acetyltransferase (CAT) reporter plasmid. The resulting plasmid was named pCAT3bBrn3aPRO.

ONS-76 cells were plated at 2.5 x $10^5$ cells/ml, 2 ml per well in 6-well Falcon plates. 4 hours after plating, the cells were transfected using GeneJuice (EMD, VWR distributor). GeneJuice transfections were optimized for ONS-76 cells to 6.5 µl of GeneJuice to 3.1 µg DNA total. The protocol was followed as per manufacturers suggestions. DNA concentrations for transfection were 0.1 µg of reporter plasmid

(pCAT3bATF6, pCAT3bBrn3aPRO), 0.5 µg pCMV-BGal, and 2.5 µg of pcDNA, pcLuS2210p, or pcZhangfei (pcZF) per tube. After transfection, cells were incubated for 48 hours in the $CO_2$ incubator. Next, CAT levels were measured using an ELISA kit (Roche Applied Science, Indianapolis, IN, USA). The CAT assay was performed in triplicate for each test group. Absorbance values for the CAT assay were measured at 410 nm (reference 490 nm). The entire experiment was repeated 2 more times to ensure reproducibility. All CAT values were normalized for transfection efficiency using β-galactosidase expression values. β-galactosidase expression was detected by the addition of *ortho*-Nitrophenyl-β-galactoside (ONPG) substrate to cell lysates, resulting in the production of a yellow pigment that can be measured at 410 nm. The amount of yellow pigment produced directly relates to the amount of β-galactosidase expressed in the cells, and therefore the transfection efficiency.

## Chapter 3: Results

### 3.1 Characterization of Zhangfei-Expressing Cells

To confirm previous results that showed a marked decrease in the growth rate of Zhangfei-expressing ONS-76 cells (143), I examined the characteristics of these cells and cells expressing the control protein β-galactosidase (LacZ) utilizing adenovirus vectors as an expression system. Figure 3.1(a) shows that ONS-76 cells expressing LacZ grew to confluency with very few floating cells 48 hours after infection. The cells were epithelial in appearance as is characteristic of ONS-76 cells. Zhangfei-expressing cells had a very different morphology. At 48 hours, some cells remained attached to the culture dish, stopped dividing and grew neurite-like projections. Other cells lost attachment to the substratum and rounded up. By 96 hours post infection, almost all cells expressing Zhangfei had detached from the culture plate. Figure 3.1(b) is a magnified view of the neurite-like projections produced by ONS-76 cells expressing Zhangfei.

The growth rates of Zhangfei and LacZ-expressing cells were examined by staining them with WST-1. In this assay, absorbance of the culture medium at 450 nm is an indication of cell number and viability (Figure 3.1c). ONS-76 cells expressing Zhangfei exhibited a drastically reduced proliferation rate and viability. Cells expressing the control protein continued to proliferate over 96 hours.

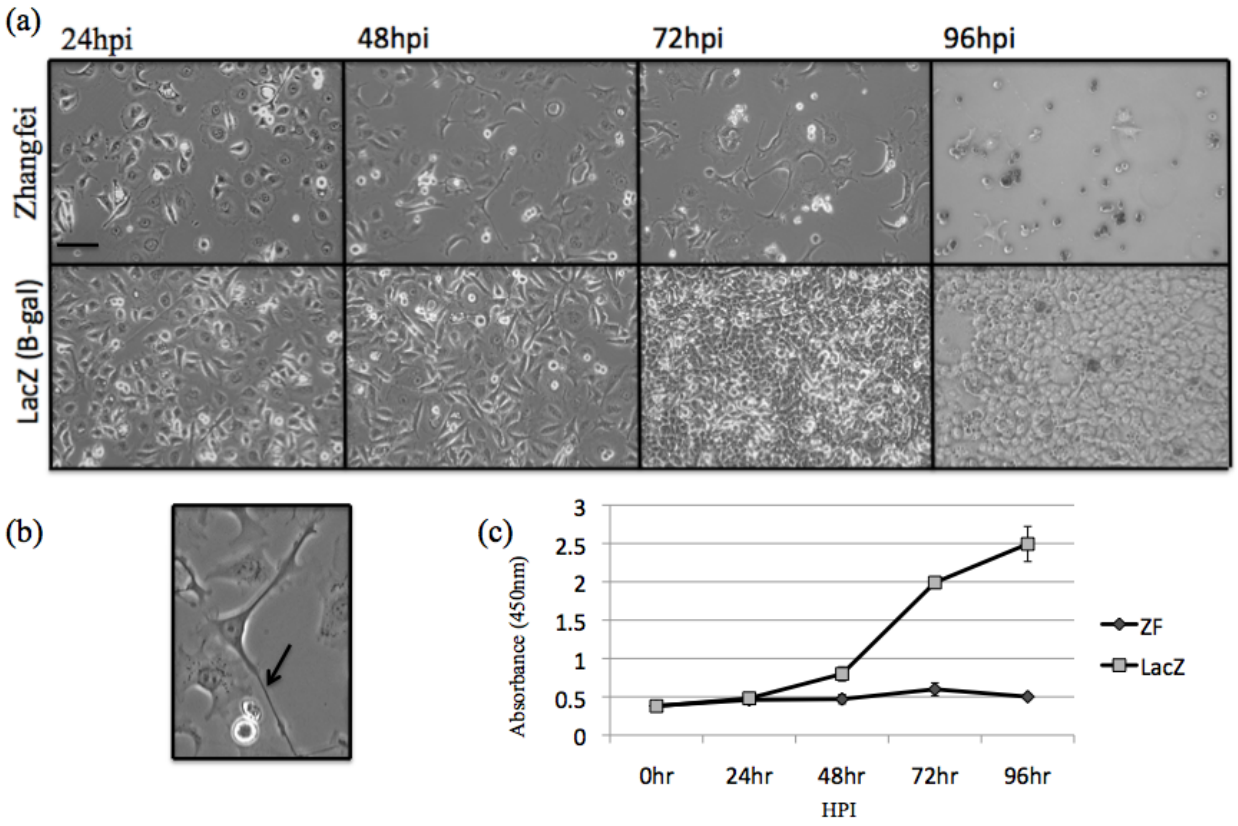


**Figure 3.1. Characterization of Zhangfei-Expressing Cells.** ONS-76 cells were examined after infection with adenovirus vectors expressing either Zhangfei or the control protein LacZ. (a) Phase contrast micrographs showing morphology of ONS-76 cells expressing either Zhangfei or LacZ. Scale bar: 100 µm. (b) Close-up of cell with neurite-like projections (arrow), 48 hpi with an adenovirus vector expressing Zhangfei. (c) Proliferation of Zhangfei and LacZ-expressing cells over time. Cells expressing Zhangfei or LacZ were stained with WST-1 on successive days after infection with adenovirus vectors and absorbance of the culture supernatant was measured.

## 3.2 Mechanisms of Cell Death

### 3.2.1 Zhangfei-Mediated Apoptotic Death of ONS-76 Cells

Cell death is characterized by oncosis or programmed cell death by apoptosis, autophagy, or macropinocytosis as reviewed by Edinger *et al.* and Overmeyer *et al.* (31, 102). To understand more about the mechanism by which Zhangfei activates cell death in ONS-76 cells, I examined cells 48 hours post infection (hpi) with Zhangfei or LacZ-expressing adenovirus vectors for markers of apoptosis, autophagy and macropinocytosis.

Phosphatidylserine exposure to the outer leaflet of the plasma membrane is a characteristic sign of apoptosis. Annexin V is a cellular protein that has a binding affinity for phosphatidylserine. Figure 3.2(a) shows the results of an Annexin V / propidium iodide staining experiment on ONS-76 cells expressing either Zhangfei or LacZ. At 48 hpi, 12.5% of cells expressing Zhangfei were pre-apoptotic and 3.4% of cells stained with propidium iodide and were considered to be dead (compared to LacZ-expressing cells at 0.23% and 0.27% respectively).

Analysis of apoptosis by fluorescent microscopy (Figure 3.2b) was performed using a Hoechst 33342 (blue) and propidium iodide (red) dual staining kit. Hoechst 33342 binds to DNA. When bound to condensed chromatin, another characteristic of cells undergoing apoptosis, it fluoresces more brightly. Propidium iodide is only permeable to dead cells. Cells could be divided into three groups based on their staining characteristics: alive, dead, or apoptotic. Three cell groups have been stained in Figure 3.2(b): β-galactosidase expressing cells which showed little variance in Hoechst 33342

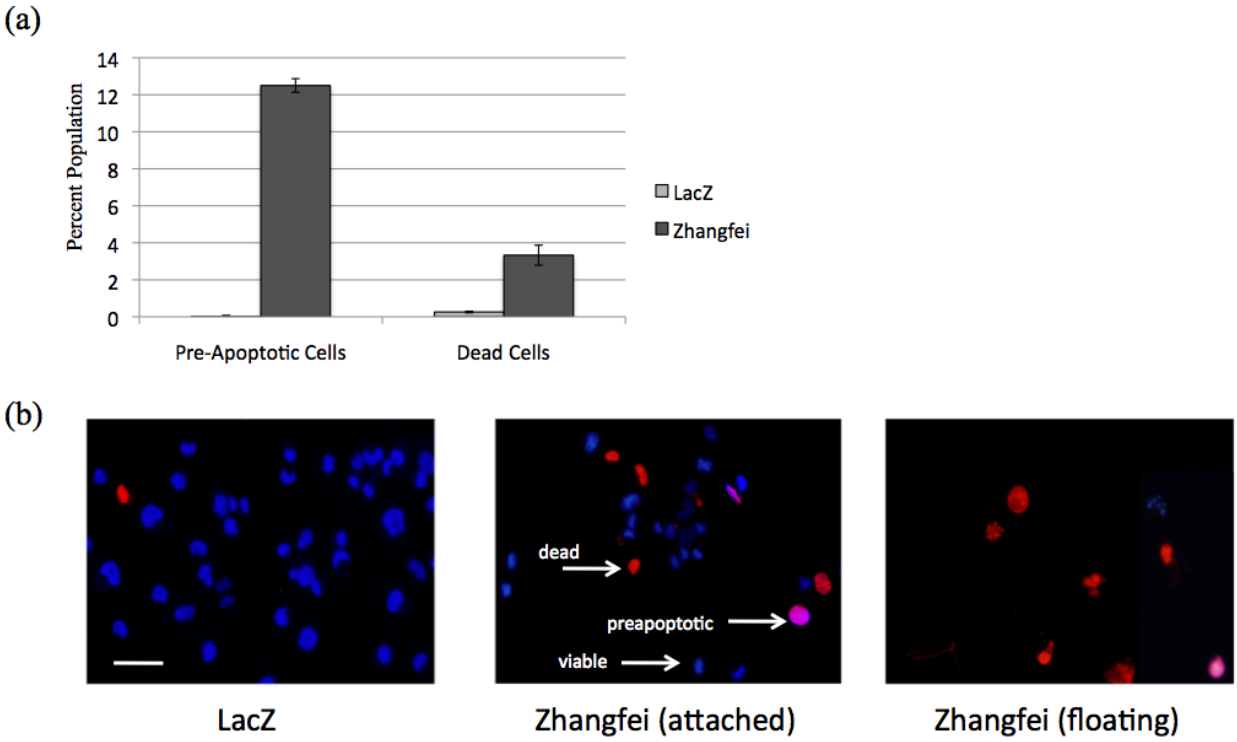


**Figure 3.2. Zhangfei-Mediated Apoptotic Death of ONS-76 Cells.** ONS-76 cells were examined 48 hpi with adenovirus vectors expressing either Zhangfei or LacZ. (a) Annexin V and propidium iodide staining of ONS-76 cells expressing either Zhangfei or control protein LacZ analyzed by flow cytometry (n = 3). Cells were grouped based on viability: preapoptotic or dead. Preapoptotic and dead cells are displayed in the figure based on percent of total cells (alive and dead). Error bars represent standard deviation. (b) Chromatin condensation analysis by fluorescence microscopy. Hoechst 33342 (blue) stains condensed DNA more brightly than uncondensed DNA. Propidium iodide (red) is permeable only to dead cells. Scale bar: 100 μm.

staining and contained few dead cells, Zhangfei-expressing cells (attached to the substratum) showing more dead and apoptotic cells than the control, and Zhangfei-expressing cells that have lost attachment to the substratum, which present with many dead cells and some apoptotic cells.

### 3.2.2 Zhangfei-Mediated Autophagic Death of ONS-76 Cells

Flow cytometry staining for autophagy was performed with the use of Cell-ID (green) stain (Figure 3.3a). Cell-ID stains autophagic vesicles. Tamoxifen was used as a positive control. Tamoxifen works by increasing intracellular ceramide levels and abolishing the inhibitory effect of class-I phosphoinositide 3′-kinase (PI3K) (124). Zhangfei expression in ONS-76 cells increased the X-mean (average Cell-ID fluorescence of the population of cells) by approximately 2-fold. Tamoxifen increased the X-mean by approximately 2.5-fold.

Fluorescent microscopy was performed using the Cell-ID stain, in conjunction with Hoechst 33342, Figure 3.3(b). Tamoxifen treated cells had bright green, peri-nuclear staining of autophagosomes. ONS-76 cells expressing LacZ had relatively few, small autophagosomes. Cells expressing Zhangfei were divided into 2 groups, cells that remained attached to the substratum at 48 hours, and cells that were floating. Many floating cells showed a fragmented nucleus (as seen by Hoechst 33342 staining), and large autophagosome compartments. Some attached, Zhangfei-expressing cells also displayed a fragmented nucleus, and interestingly, the entire cytoplasm stains a faint green. These cells failed to exhibit numerous large autophagic vesicles.

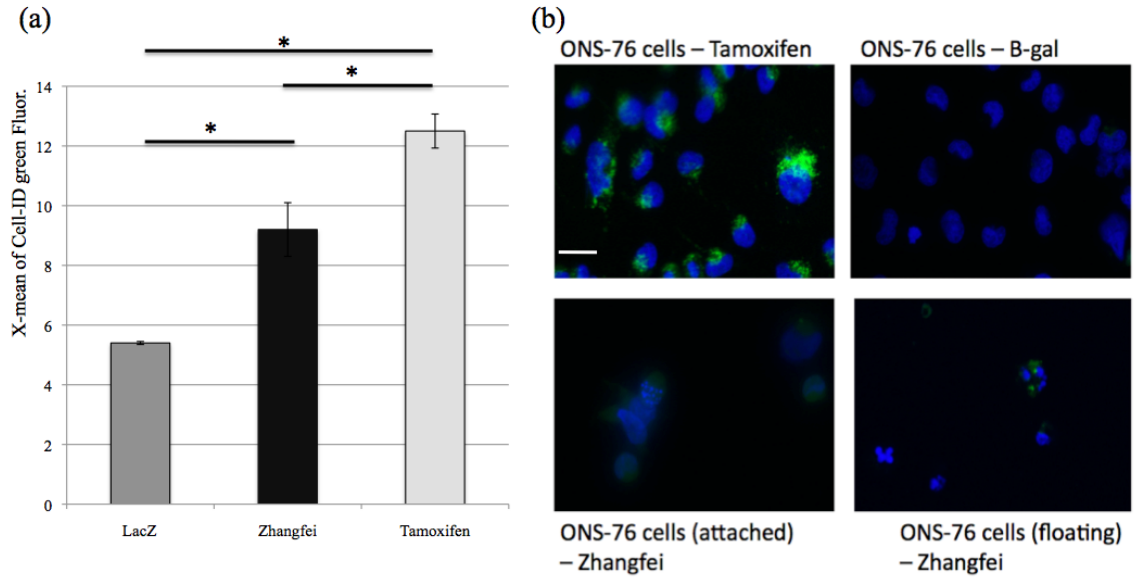


**Figure 3.3. Zhangfei-Mediated Autophagic Death of ONS-76 Cells.** ONS-76 cells were examined 48 hpi with adenovirus vectors expressing either Zhangfei or LacZ. (a) Cell-ID (green) staining of ONS-76 cells expressing either Zhangfei or LacZ analyzed by flow cytometry (n = 3). Cell-ID stains mature autophagic vesicles. X-mean refers to the average fluorescence of the entire population of cells. Tamoxifen, a chemical inducer of autophagy, was used as a positive control. A Kruskal-Wallis test of all three samples yielded a significance of >0.05. Mann-Whitney tests between treatment groups yielded significance values of >0.05. Error bars represent standard deviation. (b) Cell-ID and Hoechst 33342 staining of ONS-76 cells by fluorescent microscopy. Hoechst 33342 is used as a nuclear counter stain. Scale bar: 50 μm.

### 3.2.3 Zhangfei-Mediated Macropinocytotic Death of ONS-76 Cells

Macropinocytosis as a death pathway is characterized by the accumulation of many, large vacuoles consisting of extracellular fluids (102). To test Zhangfei-expressing ONS-76 cells for these vacuoles, the cells were stained with Alexa 488-dextran (green) and Lysotracker (red). Alexa 488-dextran supplemented in the media is taken up by cells during the normal process of macropinocytosis. If the macropinocytosis pathway is overactive, Alexa 488-dextran accumulates in enlarged vacuoles, while lysotracker red will stain lysosomes. D17 dog osteosarcoma cells were used as a positive control as they express many, large extracellular-fluid filled vesicles when they express Zhangfei (manuscript in preparation). Figure 3.4 shows that, as expected, the positive control D17 cells produced large extracellular-fluid filled vacuoles. LacZ-expressing ONS-76 cells had a few, small macropinosomes, some associated with lysosomes. Zhangfei-expressing ONS-76 cell (both floating and attached) also expressed macropinosomes, but unlike the Zhangfei-expressing D17 cells, they were small and appeared to be part of the "normal" cellular substructure.

## 3.3 Molecular Effects of Zhangfei

### 3.3.1 Zhangfei-Induced Transcription

Due to the observed involvement of Zhangfei in the processes of apoptosis, autophagy, and neurogenesis, qRT-PCR was performed to assay genes affected by

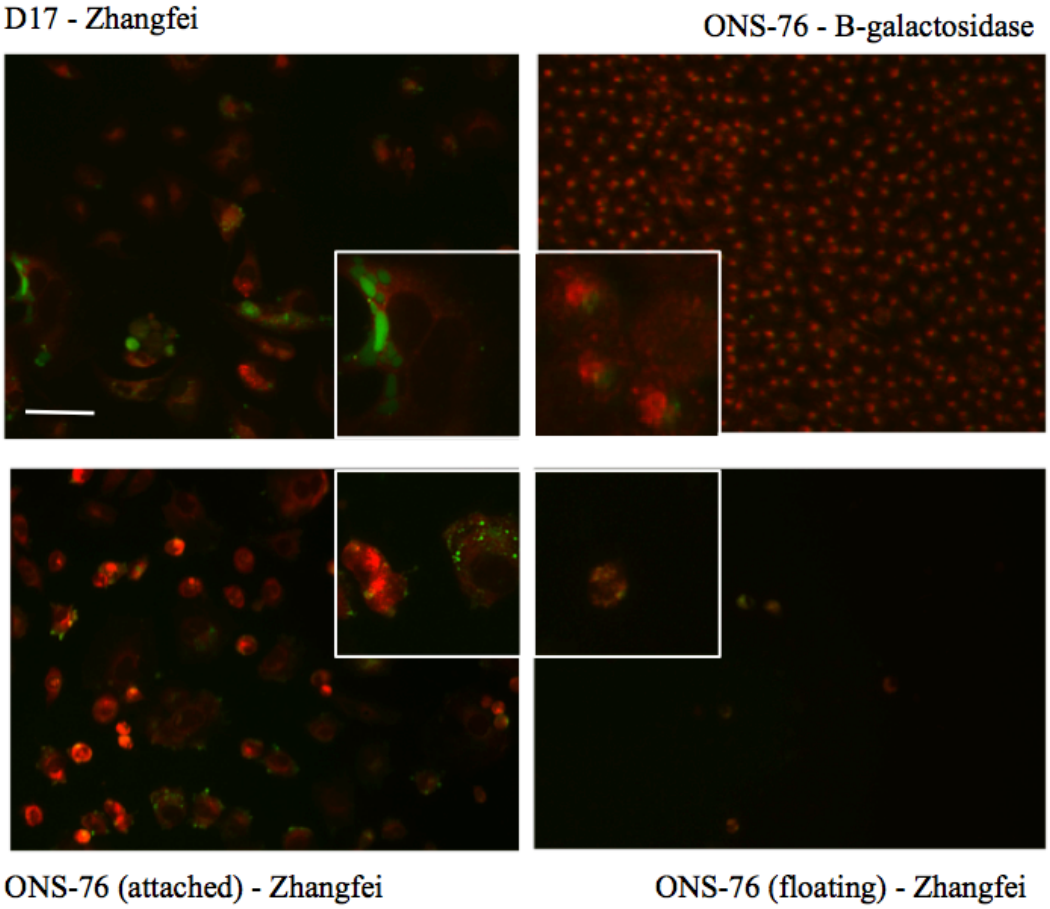


**Figure 3.4. Zhangfei-Mediated Macropinocytosis in ONS-76 Cells.** 48 hpi with adenovirus vectors expressing either Zhangfei or LacZ, ONS-76 cells were stained for macropinosome and lysosome expression. Alexa 488-dextran staining of ONS-76 cells expressing either Zhangfei or LacZ by fluorescent microscopy. D17 cells were used as a positive control as they produce large extracellular-fluid filled vesicles when they express Zhangfei. Scale bar: 100 µm. Magnified images are in insets.

Zhangfei in these three areas. To determine which cellular differentiation and apoptotic genes Zhangfei might activate in ONS-76 cells, two quantitative real time polymerase chain reaction (qRT-PCR) arrays were performed. These arrays contain 84 primer pairs for genes involved in apoptosis or neurogenesis. A 4-fold increase/decrease in gene transcript and a P-value of 0.05 or less were used to exclude transcripts that may be too low in statistical significance. The array results were subject to confirmation using qRT-PCR with primers designed in-lab.

Results from the Neurogenesis array (Figure 3.5a, top panel) indicated a number of gene transcripts were upregulated post-Zhangfei expression. These genes (indicated from most-to-least upregulated) included: amyloid beta precursor binding protein 1 (APBB1), epidermal growth factor (EGF), disk large homolog 4 (DLG4), bone morphogenic protein 8 B (BMP8B), S100 calcium binding protein B (S100B), and anaplastic lymphoma receptor tyrosine kinase (ALK). Glial cell derived neurotrophic factor (GDNF) was the only downregulated transcript. RT-PCR confirmation (figure 3.5a, bottom panel) ensured the qRT-PCR array results.

Results from the apoptosis array (Figure 3.5b) indicated that gene transcripts: tumor necrosis factor receptor superfamily member 9 (TNFRSF9), tumor necrosis factor receptor superfamily member 5 (CD40), and tumor necrosis factor (TNF) were upregulated. Gene transcripts down-regulated greater than a fold-change value of 4 include: caspase family member 1 (CASP1), and cell death-inducing DFFA-like effector A (CIDEA). Following qRT-PCR array analysis, qRT-PCR confirmation of the upregulated and downregulated gene transcripts using independently designed primers

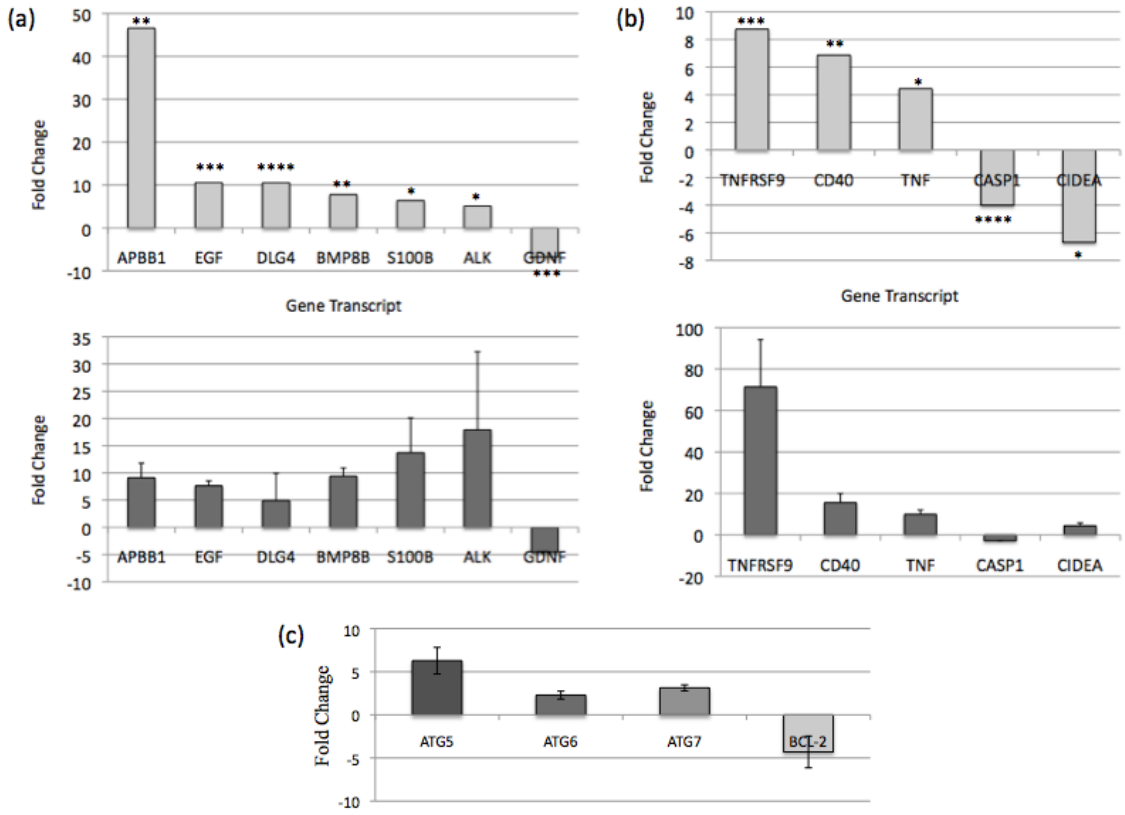


**Figure 3.5. Zhangfei-Induced Transcription.** 48 hours post-adenovirus infection, ONS-76 cells were assayed for gene transcript level changes in the areas of neurogenesis, apoptosis, and autophagy. Zhangfei-expressing cells were examined relative to control protein (LacZ) expressing cells. Each array was repeated three times and the results are shown as an average of the three. P-values for all transcripts listed (tested by qRT-PCR array, figures (a) and (b), upper portion) are all below 0.05 and are listed in the supplementary data (S1 and S2). P-values: **** (<0.0001), *** (<0.001), ** (<0.01), * (<0.05). A confirmation of gene transcript from the array displaying a fold change of greater than 4 and a P-value of less than 0.05 was performed using primers designed in-lab (n = 3). Results from the confirmation are listed directly below the array data. Bars represent standard deviation. (a) Neurogenesis cDNA array. qRT-PCR analysis of gene transcripts affected by Zhangfei expression. (b) Apoptosis cDNA array. qRT-PCR analysis of gene transcripts affected by Zhangfei expression. (c) qRT-PCR analysis of autophagy response genes: autophagy related 5 homolog (ATG5), Beclin 1 (ATG6), autophagy related 7 homolog (ATG7), and the autophagy regulator / pro-survival gene B-cell CCL/lymphoma 2. Fold change in transcript levels were measured 48 hpi in Zhangfei and LacZ-expressing cells. Each qRT-PCR experiment was performed 3 times, each experiment measuring gene expression in triplicate. Bars represent standard deviation.

was performed to confirm array accuracy. Results of this qRT-PCR confirmation are depicted in the bottom portion of Figure 3.5(b). The confirmation of the array data affirms the array's results in all but one transcript, CIDEA. CIDEA transcript was downregulated according to the apoptosis qRT-PCR array, and upregulated in the qRT-PCR confirmation. As such, CIDEA was excluded from this point forward. A list of all genes involved in the qRT-PCR arrays along with fold change and P-values is in the supplementary data sections S1 and S2 of this thesis.

To determine the effect of Zhangfei expression on autophagy-related gene transcripts, primers were designed for autophagy related 5 homolog (ATG5), Beclin 1 (ATG6), autophagy related 7 homolog (ATG7), and the autophagy regulator gene B-cell CCL/lymphoma 2 (BCL2). These genes were chosen as each plays a role in the different stages of autophagy. All three autophagy response genes were upregulated (measured by qRT-PCR) in response to Zhangfei (relative to LacZ-expressing ONS-76 cells), and pro-survival BCL2 (an inhibitor of autophagy, 106) transcript was downregulated, Figure 3.5(c). These data in combination with the absence of numerous, large autophagic vesicles in Zhangfei-expressing cells led to the conclusion that autophagy did not appear to be the primary mechanism of cell death in these cells, but rather, a natural part of cell death.

### 3.3.2 Kinome Analysis

To determine which protein kinase signaling cascades are active in Zhangfei-expressing ONS-76 cells, a kinome analysis was performed. Results for Zhangfei-

expressing cells were compared to LacZ-expressing cells. It should be noted that the kinome array used in this experiment was originally designed for characterizing immune responses, so the kinase targets tested were biased towards these processes. Only peptide phosphorylation values with a P-value of 0.05 or less would continue on to pathway analysis by InnateDB software. InnateDB is an online software program that inputs peptide phosphorylation values and predicts potential kinome cascades that are active or inactive within a group of cells. Table 3.6(a) shows the results of such a kinome analysis by InnateDB. Only kinase cascade pathways with a P-value of 0.025 or less are displayed. The top 4 molecular pathways predicted to be activated by Zhangfei expression in ONS-76 cells are: the JNK (JUN N-terminal kinase) cascade, MAPK (mitogen activated protein kinase) signaling cascade, TGFβ (transforming growth factor beta) signaling cascade (via TAK1, nuclear receptor subfamily 2, group C, member 2), and p53 (tumor protein 53) direct effector proteins. Table 3.6(b) lists the kinases that are known to be involved in each pathway. It should be noted that all pathway members corresponding to the JNK and TGFβ pathways are also represented in the MAPK signaling pathway. Explanations for this may be that kinase cascades often have a great deal of crosstalk, or that the implied activation of a pathway may simply be an artifact of the activation of another pathway with similar members. A supplementary table including all kinase targets tested, fold change in phosphorylation values, and P-values can be viewed in the supplementary data sections S7 and S8.

(a)

| Kinome Analysis: Zhangfei vs. LacZ Expressing ONS-76 Cells | | | | | |
|---|---|---|---|---|---|
| **Pathway** | **Database** | ↑ | *p* | ↓ | *p* |
| JNK Cascade | 6 | 6 | 0.003 | 0 | 1 |
| MAPK Signaling | 21 | 13 | 0.015 | 6 | 0.921 |
| TGFb Signaling (via TAK1) | 7 | 6 | 0.016 | 0 | 1 |
| P53 Direct Effectors | 4 | 4 | 0.025 | 0 | 1 |

(b)

| Kinome Analysis: Zhangfei vs. LacZ Expressing ONS-76 Cells | |
|---|---|
| **Pathway** | **Pathway Member Fold Change ↑** |
| JNK Cascade | Fos<br>Jun<br>MAP2K4 (JNKK)<br>MAP3K7<br>MAPK10 (JNK3)<br>MAPK9 (JNK2) |
| MAPK Signaling (TrkA/NGF Signaling) | CRK (P38)<br>DUSP1<br>Fos<br>Jun<br>MAP2K4 (JNKK)<br>MAP3K7<br>MAPK10 (JNK3)<br>MAPK12<br>MAPK9 (JNK2)<br>NFATC2<br>PRKCA<br>PRKCB<br>Rela (NFKb3, P65) |
| TGFb Signaling (via TAK1) | Jun<br>MAP2K4 (JNKK)<br>MAP3K7<br>MAPK10 (JNK3)<br>MAPK12<br>MAPK9 (JNK2) |
| P53 Direct Effectors | CREBBP<br>DUSP1<br>EPHA2<br>Jun |

**Table 3.6. Kinome Analysis.** Kinome analysis involves measuring the phosphorylation status of key members of kinase signaling cascades. 48 hpi with adenovirus vectors expressing either Zhangfei or LacZ, ONS-76 cells were harvested for this analysis. (a) Kinase cascades active in ONS-76 cells expressing Zhangfei. All results are a comparison between Zhangfei-expressing cells and β-galactosidase (control protein) expressing cells (n = 3). Database refers to the number of protein members in the corresponding molecular pathway that are uploaded into the InnateDB software program. The "up" and "down" arrows refer to the number of pathway members that have experienced a fold increase or decrease in phosphorylation. The corresponding P-values refer to the probability that the given pathway is or is not upregulated due to the treatment (Zhangfei expression). Only pathways with a P-value of 0.025 or lower are listed in Table 3.6(a). (b) Table 3.6(b) contains the affected individual members of the pathways listed in Table 3.6(a).

### 3.3.3 Transcription Factor Profiling Array

Transcription factors usually represent the end-effectors of signaling cascades and directly regulate the transcription of target genes. Using the transcription factor profiling array, I tested for the activation of 48 well-known transcription factors and compared the results relative to a control set of cells (LacZ-expressing cells). The results listed in this section (Figure 3.7) include only transcription factors activated, or less active by a value greater than 1.5 fold. Activated transcription factors (from most to least activated) include: brain-specific homeobox/POU domain protein 3A (Brn3a), signal transducer and activator of transcription 6, interleukin-4 induced (Stat6), transcription factor AP2 (AP2), cyclic-AMP response element binding protein (CREB), activator protein 1 (AP1), CCAAT-box-binding transcription factor zeta (CBF), v-myc myelocytomatosis viral oncogene homolog associated factor X (Myc-Max), androgen receptor (AR), tumor protein 53 (p53), forkhead box H1 (FAST-1), interferon regulatory factor (IRF), myelin expression factor 2 (Mef-2), nuclear factor kappa B (NFκB), early growth response 1 (EGR), and transcription factor Sp1 (Sp1). Transcription factors found to be less active in Zhangfei-expressing cells include SATB homeobox 1 (SATB1) and serum response element (SRE) binding factors. A full list of transcription factors included in this array, along with fold activation values can be viewed in the supplementary materials provided (S9).

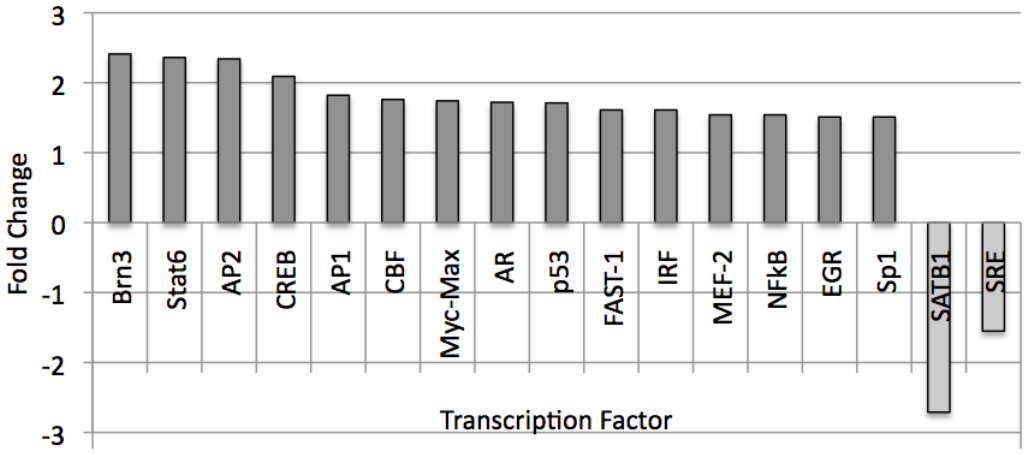


**Figure 3.7. Transcription Factor Profiling Array.** Fold activation of transcription factors in response to infection of ONS-76 cells by Adeno-Zhangfei as determined by the Signosis transcription factor profiling array (n = 1). 15 of 48 transcription factors in the array displayed a fold activation of greater than 1.5, these are displayed in the figure above. Brn3a displayed the highest value at a 2.4 fold increase in activity. A complete list of transcription factors involved in the array can be viewed in supplementary table S9. Transcription factors with a fold deactivation in activity of less than -1.5, these are SATB1 and SRE. SATB1 displayed the lowest value at a 2.7 fold decrease in activity.

## 3.4 Zhangfei, Brn3a, and TrkA: Proposing a Molecular Pathway for the Effects of Zhangfei

Based on the results of the cDNA arrays, kinome analysis, transcription factor profiling array, and previous results in our laboratory showing an increase in the expression of TrkA following the expression of Zhangfei (142), a model is proposed for the molecular mechanism by which Zhangfei may affect ONS-76 cells in Figure 3.8(a). Based on the results of the transcription factor profiling array, Zhangfei upregulates the activity of transcription factor Brn3a. Currently, Zhangfei is not known to bind any identified DNA bZIP protein recognition sites, although it may do so in conjunction with other bZIP proteins (52). Brn3a is known to regulate the expression of TrkA (80, 142). Without Zhangfei expression, TrkA expression is undetectable in ONS-76 cells. Expression of TrkA could sensitize the system to NGF stimulation, resulting in MAPK signaling (one of the top signaling pathways activated in ONS-76 cells expressing Zhangfei, according to the kinome analysis). Next, TrkA signaling could trigger the activity of downstream transcription factors and other signaling pathways that ultimately lead to the death of the ONS-76 cells. I understand that other signaling pathways may play a role in this process, but have chosen to focus in on the effects of TrkA signaling, since this offers a plausible explanation for my results.

To confirm previous results in our laboratory that TrkA transcript levels increased following Zhangfei expression in ONS-76 cells (143), primers were designed to test for TrkA transcript changes using qRT-PCR. Primers were also designed to determine

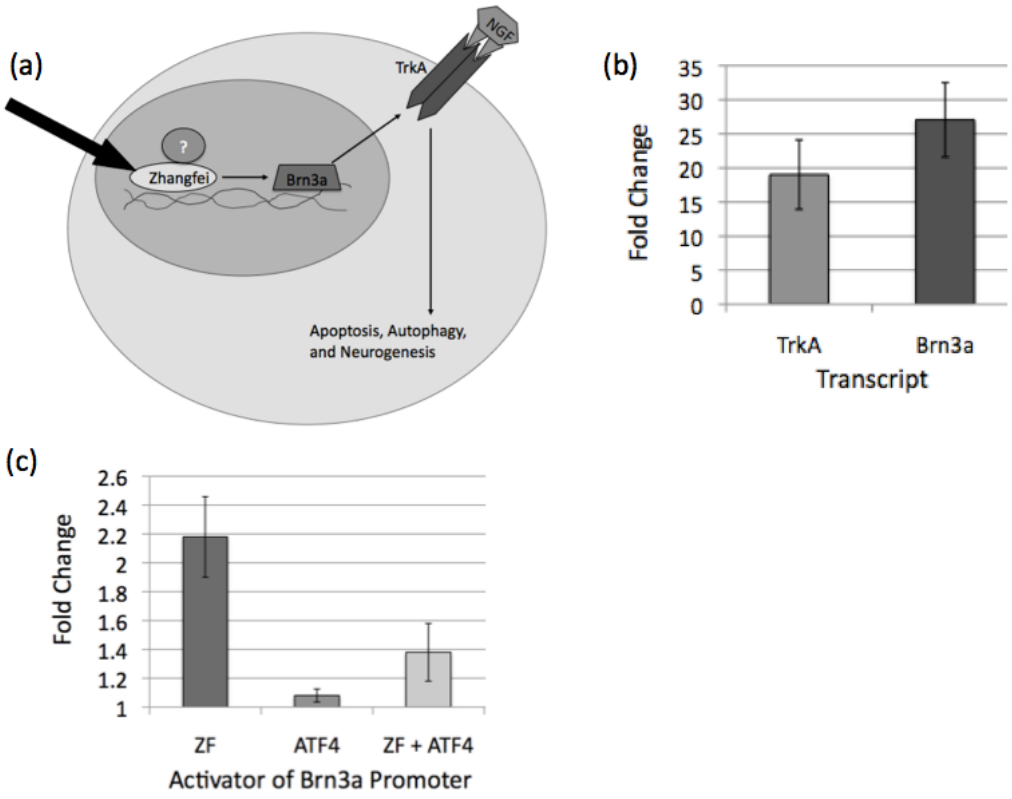


**Figure 3.8. Zhangfei, Brn3a, and TrkA: Proposing Molecular Pathway for the Effects of Zhangfei.** (a) Proposed molecular pathway for the effects of Zhangfei. A simple diagram proposing how Zhangfei may initiate cell death in ONS-76 cells. The expression of Zhangfei in ONS-76 cells mediates (perhaps with the help of another bZIP protein) the expression of Brn3a. Brn3a is a transcription factor known to be capable of inducing the expression of TrkA. I believe that TrkA signaling stimulated by autocrine NGF brings about cell death in ONS-76 cells by the activation of apoptosis with accompanying autophagy as a part of the natural death process. (b) qRT-PCR analysis of TrkA and Brn3a transcript levels (fold change), 48 hpi with adenovirus vectors expressing either Zhangfei or LacZ (n = 3). (c) The effect of Zhangfei expression on Brn3a promoter activation. A 2 kb region upstream of the Brn3a gene was isolated and cloned into a CAT expression plasmid. Next, pcZF (Zhangfei coding region cloned into pcDNA), pcATF4 (ATF4 coding region cloned into pcDNA) or a control plasmid (pcDNA) were co-transfected into ONS-76 cells. 48 hours after transfection, CAT expression levels were measured. Transfection efficiency was normalized using a β-galactosidase expressing plasmid. Zhangfei was consistently able to induce transcription from the Brn3a promoter by ~2 fold. The CAT assay results are an average of 3 assays, each containing intra-experimental duplicates. Results are displayed as fold change (CAT activation / CAT value for pcDNA).

relative levels of the Brn3a transcript. cDNA from ONS-76 cells expressing either Zhangfei or LacZ was collected 48 hpi. Brn3a was tested because it was the most upregulated transcription factor (by activity) according to the transcription factor profiling array (and a vital part of the proposed hypothesis). The results of qRT-PCR testing of these transcripts can be seen in Figure 3.8(b). TrkA transcript was upregulated by ~18 fold in Zhangfei-expressing cells, and Brn3a by ~26 fold.

Next, I explored the mechanism by which Zhangfei activates the expression of Brn3a. A 2 kb region upstream of the Brn3a gene was isolated and cloned into a CAT reporter plasmid. By measuring CAT expression with and without a co-expression of Zhangfei, the ability of Zhangfei to activate Brn3a transcription could be quantified. Results indicate that Zhangfei successfully and consistently increased transcription from the Brn3a promoter by 2.2 +/- 0.28 fold (Figure 3.8c). Co-expression of Brn3a promoter-CAT reporter (pCAT3bBrn3aPRO) and pcATF4, a plasmid expressing another bZIP containing protein, activating transcription factor 4 resulted in an increase of 1.38 +/- 0.20 fold. On its own, ATF4 was not able to activate transcription from the Brn3a promoter.

### 3.5 Nerve Growth Factor Production by ONS-76 cells

To substantiate the hypothetical pathway proposed in Figure 3.8(a), an investigation into key nodes of the pathway was initiated. NGF stimulation is characteristically the initiating step in TrkA signaling. Since it does not appear that NGF is highly upregulated in Zhangfei-expressing cells, a NGF bioassay was performed using

PC12 cells to test for NGF production. In the presence of NGF, PC12 cells grow neurites. The number of PC12 cells expressing neurites is roughly proportional to the amount of NGF administered (Figure 3.9a). ONS-76 supernatant was collected at 48 hpi with adenovirus vectors expressing either Zhangfei or LacZ. Anti-NGF antibody was used to neutralize the effects of NGF. As seen in Figure 3.9(b), anti-NGF antibody was successful in reducing the number of PC12 cells producing neurites in all three test groups by approximately 50%. Control refers to PC12 cells receiving 50 ng/ml NGF. PC12 cells receiving supernatant from LacZ-expressing cells had more cells with neurites than PC12 cells receiving supernatant from Zhangfei-expressing cells. This is not surprising, as by 48 hpi, Zhangfei-expressing cultures have much fewer cells than LacZ-expressing cultures, and are not actively proliferating.

A WST-1 proliferation and viability stain was performed on ONS-76 expressing Zhangfei or LacZ 48 hpi, as in Figure 3.9(c), but this time the growth media was supplemented with anti-NGF. Figure 3.9(c) shows how anti-NGF was able to partially restore the viability of ONS-76 cell, presumably by neutralizing the effects of NGF signaling.

### 3.6 The Effect Chemical Inhibitors on the Viability of ONS-76 Cells Expressing Zhangfei

A WST-1 proliferation and viability assay was performed on ONS-76 cells expressing Zhangfei or LacZ 48 hpi (Figure 3.10). This time, the cells were given a

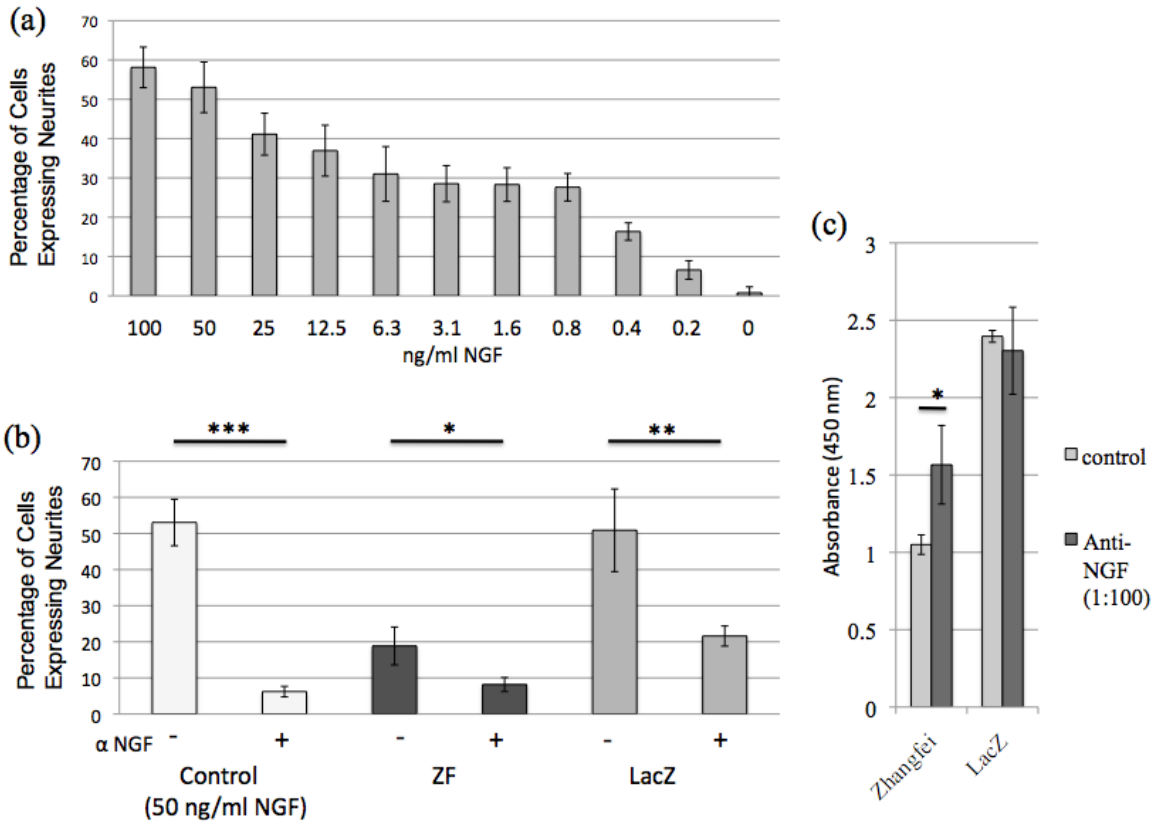


**Figure 3.9. NGF Production by ONS-76 Cells.** In the presence of NGF, PC12 cells grow neurites. PC12 cells were given supernatant from Zhangfei-expressing or LacZ-expressing ONS-76 cell cultures (48 hpi), as well as 50 ng/ml NGF as a positive control. Treatments were given with or without anti-NGF. Cells expressing neurites were counted in 10 random microscope fields at 25x objective. Anti-NGF antibody was used to neutralize the effects of NGF. (a) PC12 cell neurite growth response NGF. The bar graph created reflects the percentage of PC12 cells expressing neurites in response to various known amounts of NGF. The number of cells expressing neurites is proportional to the amount of NGF administered. (b) Neutralizing the effects of NGF. Anti-NGF antibody was able to greatly reduce the number of neurite producing cells in all three PC12 cell test groups (Zhangfei supernatant, LacZ supernatant, and 50 ng/ml NGF), (n = 3). P-values: * (< 0.05). ** (< 0.005), *** (< 0.0005). Statistical differences between samples were calculated using Student T-test. Error bars represent standard deviation. (c) Neutralization of NGF increased the viability of ONS-76 cells expressing Zhangfei. 48 hpi with adenovirus vectors expressing Zhangfei or LacZ a WST-1 staining was performed to assess the viability of these cells. Absorbance at 450 nm indicated that anti-NGF was able to partially restore the viability of Zhangfei-expressing ONS-76 cells, and have little-to-no effect on control cells. P-value: * (<0.05). Statistical differences between samples were calculated using Student T-test. Error bars represent standard deviation.

range of chemical inhibitors or left untreated as a control. This list of inhibitors selected for the analysis was based on the results of the transcription factor profiling array, kinome analysis, and work done by other researchers in the field of apoptosis and autophagy. Inhibitors used include: JNK inhibitor (i) (SP600125, 25 μM), p53i (Pifithrin alpha, 25 μM), Meki (PD98059, 50 μM), CK1i (D4476, 40 μM), apoptosis I (M50054, 420 μM), TrkAi (EMD TrkA inhibitor, 25 μM), and an ERKi (ERK inhibitor #2, EMD, 25 μM). A list of concentrations and scientific names is included in the materials and methods section (Table 2.1). The chemical inhibitors were being used in an attempt to ablate the death signaling occurring after expression of Zhangfei.

Most of the inhibitors also suppressed the growth of LacZ-expressing cells. For this reason, instead of displaying absolute absorbance values, the results were expressed as a ratio of absorbance of LacZ:Zhangfei-expressing cells, assuming that the toxic effects of the inhibitors would be the same for both cells. The ratio for untreated cells was about 2. If an inhibitor were able to completely counteract the effects of Zhangfei, the ratio would be 1. Inhibitors with ratios that were significantly different from untreated cells were JNK, MEK, and TrkA. These results suggest that JNK, MEK, and TrkA signaling play a role in Zhangfei-mediated cell death.

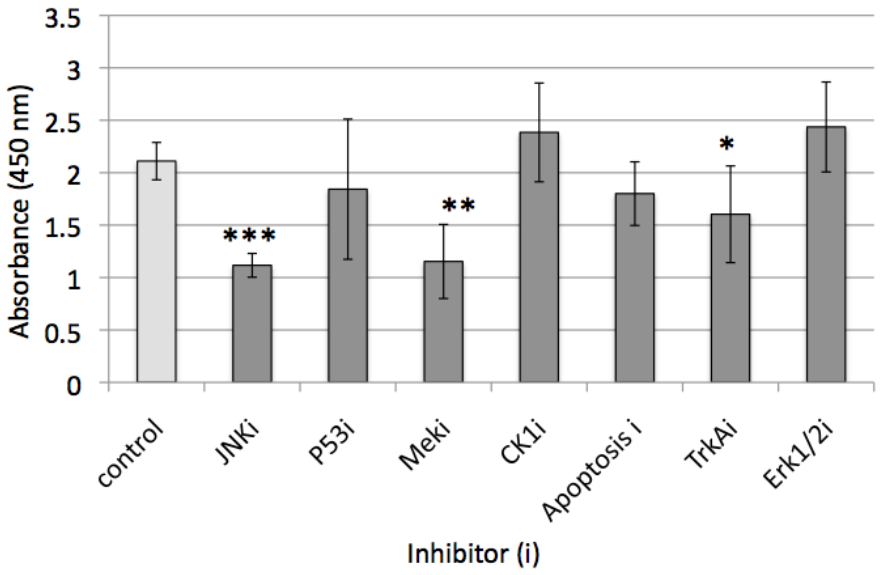


**Figure 3.10. The Effect of Chemical Inhibitors on the Viability of ONS-76 Cells Expressing Zhangfei.** After treating Zhangfei and LacZ-expressing cells with chemical inhibitors of select kinases, a WST-1 assay was performed at 48 hpi. Ratios between Zhangfei-expressing and LacZ-expressing absorbance values were taken, and the experiment was performed four times (n = 4). Ratios were used to display the results of inhibitors that were able to bring the viability of cells expressing Zhangfei to the level of cells expressing LacZ. Therefore, inhibitor groups with ratios closest to 1 were able to at least partially restore the viability of Zhangfei-expressing cells. The JNK, MEK, and TrkA inhibitors met this criterion with reasonable consistency. P-values: * (< 0.05). ** (< 0.005), *** (< 0.0005). Error bars represent standard deviation.

# Chapter 4: Discussion

## 4.1 Proposed Mechanism of Zhangfei-Induced Cell Death

### 4.1.1 Introduction

Signaling through the high-affinity nerve growth factor receptor, TrkA, is known to play a major role in the maintenance, survival, and development of sensory neurons (6, 54, 105, 128). There is evidence, however, that TrkA signaling can also play a role in the induction of cell death in neuronal tumors such as neuroblastoma and medulloblastoma. Three cellular death pathways that appear to be activated by TrkA in these neuronal tumors emerge in the literature: apoptosis, autophagy, and macropinocytosis (48, 72, 118).

### 4.1.2 Zhangfei Activates Apoptotic Cell Death With Accompanying Autophagy

Results of the fluorescent staining of ONS-76 cells expressing Zhangfei indicated a lack of numerous large macropinosomes (Figure 3.4), a feature characteristic of death brought upon by overactivation of macropinocytosis (72). As such, I concluded that Zhangfei did not overactivate macropinocytotic pathways. In addition to a lack of macropinosomes, Zhangfei-expressing cells failed to produce large, mature, perinuclear autophagosomes, a characteristic of cells undergoing autophagy as a death pathway (48). Zhangfei expression did however, increase staining of autophagic vesicles (by flow

cytometry, Figure 3.3a) and the expression of autophagy response genes ATG5, ATG6, and ATG7. These results led me to conclude that Zhangfei did not overactivate autophagic pathways in ONS-76 cells, but rather, autophagy occurred as a consequence of cell death induced by other mechanisms. The analysis of apoptosis was different. Expression of Zhangfei increased the amount of phosphatidylserine exposed to the outer leaflet of the plasma membrane (a key sign of apoptosis, Figure 3.2) in a portion of cells. Many of these cells also stained in higher amounts for condensed chromatin, another sign that apoptosis had occurred. In addition to these results, Zhangfei upregulated apoptotic response genes: TNFRSF9 (4-1BB, CD137), CD40 (TNFRSF5), and TNF (Figure 3.5b). TNFRSF9 is generally expressed in activated T-cells, B-cells, macrophages and dendritic cells (16, 28). Information on TNFRSF9 signaling is scarce, but it has been shown to link to JNK signaling (16), the most likely kinase cascade active in Zhangfei-expressing ONS-76 cells, predicted by the kinome analysis (Table 3.6a). CD40 is also known to be present on antigen-presenting cells, and is linked to JNK signaling (130, 149). The role of these membrane receptors, generally requiring activation by interaction with other immune cell ligands, remains unknown in these ONS-76 cells for the time being. In contrast, the role of TNFα in inducing apoptosis has been well documented (112). Two receptors for TNF exist, TNF-R1 and TNF-R2. TNF-R1 is expressed in most cell types, while TNF-R2 is limited to immune cells. TNF-R1 signaling is generally involved in apoptotic signaling, including cell death mediated by the JNK signaling pathway (19, 40).

Although Figure 1.3 (Literature Review) lists caspase 3 as a chief convergence point in the activation of all apoptotic events, caspase 3 transcripts were not found to be actively upregulated in Zhangfei-expressing cells. However, this may not be essential as

caspases exist as translated procaspases within the cell, and are activated by proteolytic cleavage. There have been studies however, that explore apoptosis in the absence of caspase 3 activation. Notably, Didenko *et al.* describe a situation in which TGFβ signaling leads to apoptosis in the absence of caspase 3 (14). Interestingly, TGFβ signaling was predicted to be one of the possible kinase cascades active in Zhangfei-expressing cells (Table 3.6a). TGFβ signaling may provide an explanation for the observation of caspase 3-independent apoptosis as well. In regards to autophagy accompanying apoptosis, there are many documented cases of these processes occurring in parallel (7, 27, 31, 71, 81).

### 4.2 Zhangfei and Neuronal Differentiation

When Zhangfei was expressed in ONS-76 cells, the cells stopped dividing and grew projections resembling neurites (visible at 48 hpi, Figure 3.1a, Figure 3.1b). By 96 hpi, most of the Zhangfei-expressing cells were dead. In contrast, cells expressing the control protein LacZ grew to confluency. I hypothesized that TrkA expression was at least partly responsible for the growth of the neuronal projections as TrkA signaling has been shown to play a major role in the differentiation and development of neurons (see section 1.1.6 of the Literature Review). In addition to stimulating the growth of neurite-like projections, Zhangfei was also able to increase the expression of genes involved in neurogenesis. These genes included: amyloid beta (A4) precursor binding protein (APBB1, FE65), epidermal growth factor (EGF), disks large homolog 4 (DLG4), bone morphogenic protein 8b (BMP8B), S100 calcium binding protein B (S100B), and

anaplastic lymphoma receptor tyrosine kinase (ALK). APBB1 is an adapter protein for APP (amyloid precursor protein) and is involved in regulating APP-induced transcription, DNA damage responses, upregulating apoptosis, and in neurite genesis (97). Sabo *et al.* have shown APBB1 and APP to localize in neurite growth cones of neurites and suggest that these proteins play a role in cell movement and neurite growth (120). EGF is a signaling molecule. Like NGF, EGF signaling also triggers MAPK pathway signaling. Unlike NGF signaling, EGF signaling is not usually recognized for inducing neurite growth, although Mark *et al.* have shown EGF and potassium chloride treatment of PC12 cells to stimulate neurite growth (85). Traverse *et al.* have also described a system in which EGF treatment of PC12 cells that overexpress the EGF receptor undergo differentiation (138). DLG4 interacts with other DLG proteins to form multimeric scaffolds to link ion channels and receptors (78). Although the effects of BMP8b have not been heavily studied, the BMP family of proteins are known to be highly involved in neuronal development and differentiation (88). S100B is a known negative regulator of p53, a tumor suppressor protein found to be upregulated in activity by the transcription factor profiling array (Figure 3.7). S100B has been shown to either promote neurite growth and cellular survival or promote apoptosis in a dose dependent manner (117). S100B is generally secreted by glial cells, targeting neurites. S100B secretion may represent the bipotential differentiation of ONS-76 cells to both neuronal and glial cells. ALK is a tyrosine receptor kinase, like TrkA. It is expressed in the developing central and peripheral nervous system. Expression of constitutively active ALK in PC12 cells resulted in neurite growth and differentiation in a MAPK signaling pathway dependent

manner (43). Altogether, these results support the hypothesis that Zhangfei activates neuronal differentiation in ONS-76 cells.

### 4.3 Molecular Mechanisms Executing the Effects of Zhangfei

Based on results obtained, a mechanism was proposed by which Zhangfei may activate apoptosis in ONS-76 medulloblastoma cells with autophagy accompanying cell death as a natural process. In this model (Figure 3.8a) Zhangfei induces the expression of transcription factor Brn3a, resulting in the transcription of TrkA. A modified version of this figure is repeated below (Figure 4.1). Figure 4.1 lists signaling pathways thought to be upregulated in Zhangfei-expressing cells, and my evidence supported each pathway. Zhangfei was able to induce expression from a CAT expression plasmid containing the Brn3a promoter, by approximately 2 fold (Figure 3.8c). Brn3a transcriptional activity was increased by approximately 2.5 fold in Zhangfei-expressing cells according to a transcription factor profiling array (Figure 3.7c). Brn3a has been proposed as a transcription factor capable of influencing TrkA expression (80, 141). Expression of both Brn3a and TrkA transcript increased by approximately 25 and 20 fold in Zhangfei-expressing ONS-76 cells, respectively (Figure 3.8b).

According to the kinome analysis, the TrkA (MAPK signaling pathway), was one of the top-four predicted signaling pathways likely to be active in Zhangfei-expressing ONS-76 cells (Table 3.6a). Initiation of MAPK signaling involves binding of NGF to the TrkA receptor. ONS-76 cells were found to produce NGF regardless of the expression of Zhangfei (ie. both control protein and Zhangfei-expressing ONS-76 cells produced NGF,

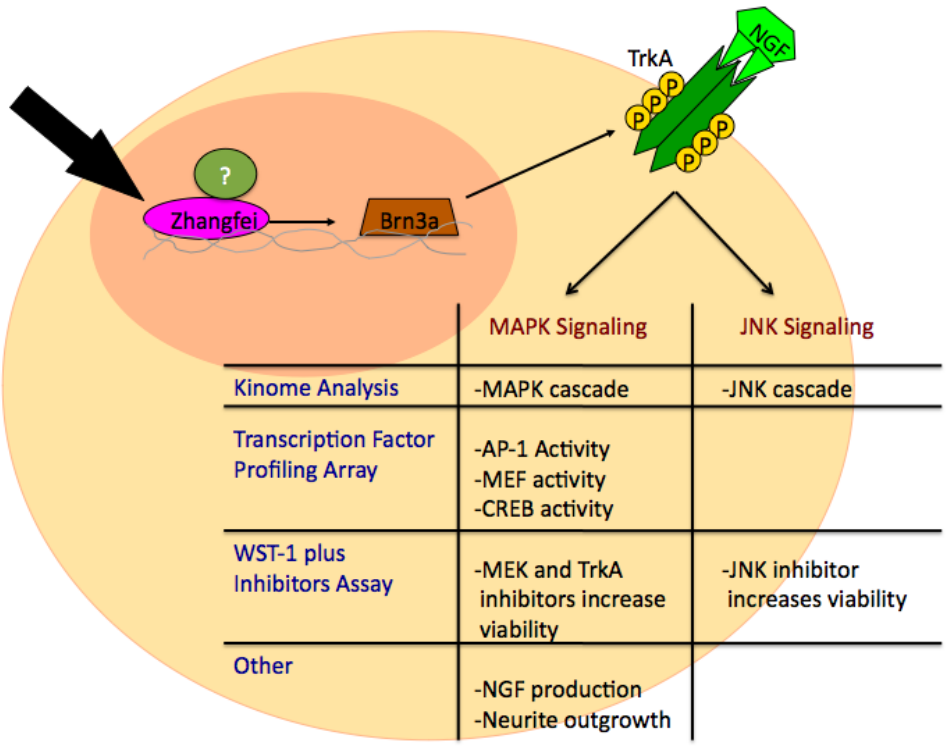


**Figure 4.1. Molecular Mechanisms Executing the Effects of Zhangfei.** Activation of MAPK and JNK Signaling Pathways by Zhangfei. Expression of Zhangfei in ONS-76 cells results in the transcription of Brn3a and TrkA. Zhangfei increased expression from the Brn3a promoter by approximately 2-fold. Brn3a, as a transcription factor, has been shown to actively upregulate TrkA expression. Activation of TrkA has been shown to increase both MAPK and JNK signaling pathways. The table listed in the figure gives experimental support to the activation of these signaling pathways in ONS-76 cells expressing Zhangfei.

Figure 3.9). LacZ-expressing cultures were found to produce more NGF than Zhangfei-expressing cells at 48 hpi with adenovirus vectors. This is not surprising as Zhangfei-expressing cells appeared to stop dividing immediately following Adeno-Zhangfei infection, while Adeno-LacZ-infected cells continued to multiply and reach a high density. Neutralization of NGF in the media of Zhangfei-expressing cells also increased the viability of these cells at 48 hpi (Figure 3.9c). This further supports the hypothesis that the TrkA pathway is activated in Zhangfei-expressing cells by autocrine NGF stimulation. Activation of the MAPK signaling pathway by TrkA-NGF interactions may lead to the activation of transcription factors c-Fos (cellular oncogene fos) and c-Jun (Jun activation domain binding protein), collectively known as AP-1. AP-1 transcriptional activity was found to be upregulated in Zhangfei-expressing cells.

After prolonged activation, TrkA is endocytosed and continues to signal. This process is termed retrograde signaling (Figure 1.2). Retrograde signaling targets transcription factors such as cyclic-AMP response element binding protein (CREB) and Myocyte enhancing factor 2 (MEF2) (114, 147), both of which expressed a higher level of activity in Zhangfei-expressing cells (2.1 and 1.5 fold increases, respectively) as discovered in the transcription factor profiling array (Figure 3.7).

In some instances, TrkA signaling has been shown to correlate with JNK activation resulting in cell death (59). In turn, JNK signaling may activate transcription factor c-Jun (56). Inhibition of JNK signaling has been shown to ablate apoptotic signaling by Bax (73). Overexpression of c-Jun and activation of JNK signaling have both been shown to increase p53 stabilization and accumulation in mouse fibroblasts (39, 70). The transcriptional activity of p53 was upregulated in Zhangfei-expressing cells

according to the transcription factor profiling array (Figure 3.7). p53 has also been linked to TrkA-induced apoptosis in neuroblastoma cells (69). p53 has been shown to directly increase the transcription of pro-apoptotic protein PUMA (BBC3) (47, 146), which in turn directly interacts (not shown) with pro-apoptotic Bax and anti-apoptotic Bcl-2 to induce cell death (90). Bcl-2 transcripts were downregulated in Zhangfei-expressing cells. Bcl-2 plays a role in inhibiting ATG6 (Beclin 1) dependent autophagy (107). Removal of the inhibitory effects of Bcl-2 may turn its role from stabilizing cellular autophagy to allowing overactivation of autophagy. Removal of Bcl-2 inhibition of Bax allows for the activation of apoptosis (101). In any case, the activation of autophagy and/or apoptosis appears to be a balancing act. Much crosstalk occurs between these two programmed cellular death pathways, as reviewed in (81).

My results support a model in which autocrine NGF-TrkA stimulation leads to the possible differentiation and eventual death of ONS-76 cells that express Zhangfei. The mechanism of cell death points to apoptosis. Autophagy accompanies cell death in what appears to be a part of the natural death process. TrkA-induced apoptosis and autophagy are frequently referenced in the studies of neurological tumors. Apoptosis appeared to be at least partially reliant on MEK, JNK, and TrkA activation. Further work must identify the DNA binding partner(s) of Zhangfei or discover the role of tumor necrosis family members in Zhangfei-induced cell death. In time, Zhangfei may also prove to be a great candidate for translational cancer research.

## Chapter 5: Supplementary Data

S1. Data from Neurogenesis qRT-PCR Array. All genes involved in the array, including P-value and Fold Regulation.

| Neurogenesis | Position | Symbol | P-Value | Fold Regulations |
|---|---|---|---|---|
| | A03 | ADORA2A | 0.134095 | 4.88 |
| | A04 | ALK | 0.030613 | 4.28 |
| | A05 | APBB1 | 0.002246 | 39.17 |
| | A10 | BAI1 | 0.063245 | 5.59 |
| | B03 | BMP8B | 0.001451 | 6.54 |
| | B10 | DLG4 | 0.000088 | 8.85 |
| | C04 | EGF | 0.000166 | 8.89 |
| | G04 | S100B | 0.015575 | 5.36 |
| | A12 | BMP15 | 0.373895 | -10.07 |
| | C08 | FGF13 | 0.133776 | -12.37 |
| | C11 | GDNF | 0.000441 | -8.05 |
| | D10 | INHBA | 0.001502 | -4.05 |
| | A01 | ACHE | 0.27484 | 3.16 |
| | A02 | ADORA1 | 0.049346 | 2.44 |
| | A06 | APOE | 0.431816 | -1.32 |
| | A07 | ARNT2 | 0.086183 | -1.56 |
| | A08 | ARTN | 0.08785 | 2.03 |
| | A09 | ASCL1 | 0.568213 | 1.28 |
| | A11 | BDNF | 0.334031 | -1.97 |
| | B01 | BMP2 | 0.8604 | 1.36 |
| | B02 | BMP4 | 0.026032 | 2.3 |
| | B04 | CDK5R1 | 0.663732 | -1.14 |
| | B05 | CDK5RAP1 | 0.978707 | 1.01 |
| | B06 | CDK5RAP2 | 0.002645 | 1.73 |
| | B07 | CDK5RAP3 | 0.50241 | 1.1 |
| | B08 | CHRM2 | 0.816317 | 1.23 |
| | B09 | CXCL1 | 0.888359 | -1.13 |
| | B11 | DLL1 | 0.002265 | -2.58 |
| | B12 | DRD1 | 0.42767 | 1.96 |
| | C01 | DRD2 | 0.571029 | -1.2 |
| | C02 | DVL3 | 0.346619 | 1.42 |
| | C03 | EFNB1 | 0.19328 | -1.9 |
| | C05 | EP300 | 0.905443 | -1.89 |
| | C06 | ERBB2 | 0.081301 | 2.36 |
| | C07 | FEZ1 | 0.002139 | -1.46 |
| | C09 | FGF2 | 0.44026 | -1.21 |
| | C10 | FLNA | 0.074127 | -2.7 |
| | C12 | GNAO1 | 0.028456 | -2.33 |
| | D01 | GPI | 0.003156 | 1.8 |
| | D02 | GRIN1 | 0.915018 | 1.03 |
| | D03 | HDAC4 | 0.038867 | 2.26 |

| | | | |
|---|---|---|---|
| D04 | HDAC7 | 0.023736 | 1.91 |
| D05 | HES1 | 0.567474 | 1.12 |
| D06 | HEY1 | 0.056637 | -3.48 |
| D07 | HEY2 | 0.763158 | 1.16 |
| D08 | HEYL | 0.327698 | 1.42 |
| D09 | IL3 | 0.901606 | 1.02 |
| D11 | MDK | 0.013283 | -3.13 |
| D12 | MEF2C | 0.72825 | -1.1 |
| E01 | MLL | 0.321081 | 1.48 |
| E02 | NCOA6 | 0.040438 | 1.77 |
| E03 | NDN | 0.092005 | -3.56 |
| E04 | NDP | 0.006592 | -2.99 |
| E05 | NEUROD1 | 0.901606 | 1.02 |
| E06 | NOG | 0.100152 | -3.02 |
| E07 | NOTCH2 | 0.442984 | -1.34 |
| E08 | NPTX1 | 0.394996 | 2.05 |
| E09 | NRCAM | 0.502812 | 1.48 |
| E10 | NRG1 | 0.037444 | -3.25 |
| E11 | NRP1 | 0.473606 | 1.19 |
| E12 | NRP2 | 0.036131 | -3.58 |
| F01 | NTN1 | 0.290834 | 1.32 |
| F02 | ODZ1 | 0.167855 | 1.26 |
| F03 | PAFAH1B1 | 0.441026 | 1.13 |
| F04 | PARD3 | 0.792798 | -1.07 |
| F05 | PARD6B | 0.002127 | 3.05 |
| F06 | PAX3 | 0.901606 | 1.02 |
| F07 | PAX5 | 0.901606 | 1.02 |
| F08 | PAX6 | 0.016455 | 2.1 |
| F09 | POU3F3 | 0.901606 | 1.02 |
| F10 | POU4F1 | 0.34516 | -1.21 |
| F11 | PTN | 0.094448 | -1.56 |
| F12 | RAC1 | 0.029686 | 1.24 |
| G01 | ROBO1 | 0.337905 | 1.27 |
| G02 | RTN4 | 0.367126 | 1.2 |
| G03 | S100A6 | 0.001077 | -1.89 |
| G05 | SEMA4D | 0.010939 | 2.16 |
| G06 | SHH | 0.004646 | -1.82 |
| G07 | SLIT2 | 0.690641 | 1.17 |
| G08 | SOX8 | 0.901606 | 1.02 |
| G09 | STAT3 | 0.099216 | 1.25 |
| G10 | TNR | 0.73432 | -1.29 |
| G11 | VEGFA | 0.976868 | -1.04 |
| G12 | YWHAH | 0.181997 | 1.32 |
| H01 | B2M | 0.01057 | 1.81 |
| H02 | HPRT1 | 0.07691 | 1.51 |
| H03 | RPL13A | 0.001555 | -2.38 |
| H04 | GAPDH | 0.003638 | -1.67 |
| H05 | ACTB | 0.112931 | -1.64 |
| H06 | HGDC | 0.567029 | 1.03 |

| | | | |
|---|---|---|---|
| H07 | RTC | 0.298577 | 1.26 |
| H08 | RTC | 0.67651 | 1.07 |
| H09 | RTC | 0.805508 | -1.13 |
| H10 | PPC | 0.384121 | -1.22 |
| H11 | PPC | 0.282891 | -1.18 |
| H12 | PPC | 0.365474 | -1.2 |

S2. Data from Apoptosis qRT-PCR Array. All genes involved in the array, including P-value and Fold Regulation.

| Apoptosis | Position | Symbol | P-Value | Fold Regulations |
|---|---|---|---|---|
| | D10 | CD40 | 0.006885 | 6.87 |
| | F06 | TNF | 0.016471 | 4.44 |
| | G02 | TNFRSF9 | 0.000933 | 8.74 |
| | C11 | CASP1 | 0.000015 | -4 |
| | E01 | CIDEA | 0.011967 | -6.69 |
| | A01 | ABL1 | 0.011676 | 1.7 |
| | A02 | AKT1 | 0.000113 | 1.86 |
| | A03 | APAF1 | 0.030334 | 1.34 |
| | A04 | BAD | 0.000602 | 2.6 |
| | A05 | BAG1 | 0.622715 | -1.03 |
| | A06 | BAG3 | 0.447659 | 1.05 |
| | A07 | BAG4 | 0.031516 | 1.44 |
| | A08 | BAK1 | 0.031049 | 1.37 |
| | A09 | BAX | 0.043794 | 1.26 |
| | A10 | BCL10 | 0.770888 | 1.11 |
| | A11 | BCL2 | 0.021578 | -1.36 |
| | A12 | BCL2A1 | 0.232434 | 1.49 |
| | B01 | BCL2L1 | 0.001461 | -1.99 |
| | B02 | BCL2L10 | 0.182863 | 1.61 |
| | B03 | BCL2L11 | 0.006876 | 1.92 |
| | B04 | BCL2L2 | 0.42448 | 1.15 |
| | B05 | BCLAF1 | 0.495807 | -1.25 |
| | B06 | BFAR | 0.471205 | -1.19 |
| | B07 | BID | 0.004213 | 2.25 |
| | B08 | BIK | 0.003272 | -1.45 |
| | B09 | NAIP | 0.071942 | 1.39 |
| | B10 | BIRC2 | 0.046717 | 1.38 |
| | B11 | BIRC3 | 0.502458 | -1.13 |
| | B12 | XIAP | 0.170154 | 1.2 |
| | C01 | BIRC6 | 0.000632 | 2.47 |
| | C02 | BIRC8 | 0.031713 | 1.25 |
| | C03 | BNIP1 | 0.393466 | 1.17 |
| | C04 | BNIP2 | 0.104713 | 1.34 |
| | C05 | BNIP3 | 0.450553 | -1.15 |
| | C06 | BNIP3L | 0.080085 | -1.12 |
| | C07 | BRAF | 0.00981 | 2.11 |
| | C08 | NOD1 | 0.064752 | 1.49 |

| | | | |
|---|---|---|---|
| C09 | CARD6 | 0.06253 | -1.61 |
| C10 | CARD8 | 0.270368 | -1.21 |
| C12 | CASP10 | 0.04806 | -1.23 |
| D01 | CASP14 | 0.031713 | 1.25 |
| D02 | CASP2 | 0.326284 | 1.1 |
| D03 | CASP3 | 0.013723 | 1.15 |
| D04 | CASP4 | 0.151276 | 1.08 |
| D05 | CASP5 | 0.245093 | -1.23 |
| D06 | CASP6 | 0.206896 | -1.15 |
| D07 | CASP7 | 0.064806 | 1.49 |
| D08 | CASP8 | 0.706153 | 1.03 |
| D09 | CASP9 | 0.004937 | 2.23 |
| D11 | CD40LG | 0.031713 | 1.25 |
| D12 | CFLAR | 0.001577 | -1.3 |
| E02 | CIDEB | 0.055223 | 1.66 |
| E03 | CRADD | 0.027705 | -1.3 |
| E04 | DAPK1 | 0.031713 | 1.25 |
| E05 | DFFA | 0.121682 | -1.32 |
| E06 | FADD | 0.044155 | 1.33 |
| E07 | FAS | 0.014663 | -1.51 |
| E08 | FASLG | 0.031713 | 1.25 |
| E09 | GADD45A | 0.007448 | -1.5 |
| E10 | HRK | 0.76486 | 1 |
| E11 | IGF1R | 0.007518 | 1.28 |
| E12 | LTA | 0.992385 | 1.13 |
| F01 | LTBR | 0.041144 | -1.45 |
| F02 | MCL1 | 0.406905 | 1.09 |
| F03 | NOL3 | 0.172055 | -1.17 |
| F04 | PYCARD | 0.126064 | 1.84 |
| F05 | RIPK2 | 0.001025 | -1.49 |
| F07 | TNFRSF10A | 0.176009 | 2.04 |
| F08 | TNFRSF10B | 0.00628 | 1.43 |
| F09 | TNFRSF11B | 0.005613 | 1.43 |
| F10 | TNFRSF1A | 0.870007 | -1.03 |
| F11 | TNFRSF21 | 0.000001 | -1.53 |
| F12 | TNFRSF25 | 0.928636 | 1.08 |
| G01 | CD27 | 0.551223 | -1.13 |
| G03 | TNFSF10 | 0.000002 | -2.79 |
| G04 | CD70 | 0.001792 | 1.72 |
| G05 | TNFSF8 | 0.031713 | 1.25 |
| G06 | TP53 | 0.094841 | 1.21 |
| G07 | TP53BP2 | 0.047614 | 1.6 |
| G08 | TP73 | 0.854236 | -1.02 |
| G09 | TRADD | 0.043231 | 1.22 |
| G10 | TRAF2 | 0.692709 | 1.04 |
| G11 | TRAF3 | 0.029393 | 1.5 |
| G12 | TRAF4 | 0.485668 | 1.08 |
| H01 | B2M | 0.001989 | 2.01 |
| H02 | HPRT1 | 0.004366 | 1.6 |

| | | | |
|---|---|---|---|
| H03 | RPL13A | 0.000009 | -2.53 |
| H04 | GAPDH | 0.788761 | -1.01 |
| H05 | ACTB | 0.261468 | -1.26 |
| H06 | HGDC | 0.333312 | -1.24 |
| H07 | RTC | 0.003204 | 1.12 |
| H08 | RTC | 0.102124 | 1.18 |
| H09 | RTC | 0.231264 | 1.13 |
| H10 | PPC | 0.424103 | 1.07 |
| H11 | PPC | 0.643606 | 1.05 |
| H12 | PPC | 0.881998 | 1 |

## S3. Primer Sequences for qRT-PCR Confirmation of Neurogenesis Array

| Gene Name | Upstream Primer ($5^1$-$3^1$) | Downstream Primer ($5^1$-$3^1$) |
|---|---|---|
| APBB1 | TCTGTTCCATCATCACTGAGC | GTTCTGGCCCTCTTTTAGCC |
| EGF | TCACCTCAGGGAAGATGACC | CAGTTCCCACCACTTCAGG |
| DLG4 | CACTCCTCACAGTGCTGCATAG | CCTGGGGCTTCTAGGGTATC |
| BMP8B | ATTGGAAGGAGTTCCGCTTTG | GTCACTGGCTGCTGTGACATC |
| ADORA2A | AGGCAGCAAGAACCTTTC | CTAAGGAGCTCCACGTCTGG |
| ALK | GCAACATCAGCCTGAAGAC | GCCTGTTGAGAGACCAGGAG |
| S100B | ATTCTGGAAGGGAGGGAGAC | CGTGGCAGGCAGTAGTAACC |
| GDNF | CCAACCCAGAGAATTCCAG | CAACATGCCTGCCCTACTTTG |
| BMP15 | GATTCCTCAAAACCTTCCCTG | CAAGAAGGCAATGTCAAGGATG |
| FGF13 | GGGTGGTATCTGGGTCTGAAC | CATTGTGGCTCATGGATTTG |

## S4. Primer Sequences for qRT-PCR Confirmation of Apoptosis Array

| Gene Name | Upstream Primer ($5^1$-$3^1$) | Downstream Primer ($5^1$-$3^1$) |
|---|---|---|
| TNFRSF9 | GTCGACCCTGGACAAACTG | TTTCTGCCCCGTTTAACAAC |
| CD40 | GCAGGCACAAACAAGACTG | TCGGGAAAATTGATCTCCTG |
| TNF | AGCCCATGTTGTAGCAAACC | GATGGCAGAGAGGAGGTTG |
| CASP2 | CTCAGGCTCAGAAGGGAATG | CGCTGTACCCCAGATTTTG |
| CIDEA | ACTCTGGTGCTGGAGGAAG | TTAAGGCAGCCGATGAAGTC |

## S5. Primer Sequences for Autophagy Response Gene Regulation

| Gene Name | Upstream Primer ($5^1$-$3^1$) | Downstream Primer ($5^1$-$3^1$) |
|---|---|---|
| ATG5 | GCAAGCCAGACAGGAAAAAG | GACCTTCAGTTGGTCCGGTAA |
| ATG6 (Beclin 1) | CAAGATCCTGGACCGTGTCA | TGGCACTTTCTGTGGACATCA |
| ATG7 | CAGGAGATTCAACCAGAGAC | AGATACCATCAATTCCACGG |
| BCL2 | TGCACCTGACGCCCTTCAC | AGACAGCCAGGAGAAATCAAACAG |

## S6. Other Primers

| | | |
|---|---|---|
| TrkA | GAGGGCAAAGGCTCTGGACTCCA | AGACTCCGAAGCGCACGATG |

| | | |
|---|---|---|
| Zhangfei | CTGACCACCTCCCTCTTCAG | CAGAACTCCACCGACACCTT |
| GAPDH | GCCTCCTGCACCACCAACTG | GGGCCATCCACAGTCTTCTGG |
| Brn3a | GGTACCTAAAGACCAGAGCTTCTTTG | CTCGAGGACGGGATGCACTCCTCTAA |

S7. Kinome Array Results. Raw Data for Adeno-LacZ-infected ONS-76 cells. P value cutoff of 0.05.

| Gene Name | Target amino acid | Genbank | ZF2/3 vs. Lac2/3 up | ZF3 vs. Lac3 down | ZF2/3 vs. Lac2/3 fold change |
|---|---|---|---|---|---|
| **EphA2** | Y772 | P29317 | 0.001182825 | 0.998817175 | 1.49736966 |
| **TAK1** | T184 | O43318 | 0.002025469 | 0.997974531 | 1.516308493 |
| **IRF-3** | S396/8 | Q14653 | 0.003606114 | 0.996393886 | 1.17174897 |
| **STAT1** | S727 | P42224 | 0.003942177 | 0.996057823 | 1.649226326 |
| **IRF-3** | S385/6 | Q14653 | 0.004410719 | 0.995589281 | 2.540041177 |
| **Crk** | Y221 | P46108 | 0.00667695 | 0.99332305 | 1.955734327 |
| **NFκB-p65** | S311 | Q04206 | 0.007252056 | 0.992747944 | 1.517852368 |
| **JNK3** | T131 | P53779 | 0.007362009 | 0.992637991 | 1.832600522 |
| **PKACa** | T195/7 | P17612 | 0.007449918 | 0.992550082 | 1.338862612 |
| **Notch 2** | S2070 | Q04721 | 0.008756818 | 0.991243182 | 1.230074244 |
| **P38 gamma** | Y323 | P53778 | 0.009783959 | 0.990216041 | 1.530096159 |
| **HSP70** | Y525/6 | P08107 | 0.012666251 | 0.987333749 | 1.662024614 |
| | | | | | |
| **PLCB1** | S887 | Q9NQ66 | 0.016572549 | 0.983427451 | 1.354325672 |
| **SEK1** | S257/0 | P45985 | 0.017410418 | 0.982589582 | 2.029644341 |
| **Grb10** | S150 | Q13322 | 0.018172481 | 0.981827519 | 2.41114841 |
| **IL-8R B** | S351/2/3 | P25025 | 0.025055239 | 0.974944761 | 2.535084431 |
| **RBL2_SYMSP** | | | 0.028253779 | 0.971746221 | 2.71942569 |
| **JNK2** | T404/7 | P45984 | 0.029525338 | 0.970474662 | 1.727325571 |
| **Fos** | T232 | P01100 | 0.029706366 | 0.970293634 | 1.504427419 |
| **STAT3** | S727 | P40763 | 0.032854427 | 0.967145573 | 1.27412846 |
| **smMLCK** | S1773 | Q15746 | 0.03313294 | 0.96686706 | 1.661472308 |
| **STAT2** | Y690 | P52630 | 0.034178239 | 0.965821761 | 1.376355601 |
| **Jun** | S63 | P05412 | 0.034736712 | 0.965263288 | 1.704580746 |
| **IL-8R B** | S347 | P25025 | 0.03512201 | 0.96487799 | 1.511224568 |
| **mucin 1** | T1224/7/9 | P15941 | 0.036684837 | 0.963315163 | 1.941291022 |
| **PKCA** | T637 | P17252 | 0.039731572 | 0.960268428 | 1.925225712 |
| **p38-alpha** | T180/2 | Q16539 | 0.041880534 | 0.958119466 | 1.162071137 |
| **LRRFIP1** | S497 | O75766 | 0.042424626 | 0.957575374 | 3.027104247 |
| **NFAT1** | S168 | Q13469 | 0.042504237 | 0.957495763 | 1.491589421 |
| **DNA-PK** | T2609 | P78527 | 0.042762478 | 0.957237522 | 1.324442277 |
| **PKCB** | S15/T16 | P05771 | 0.04567759 | 0.95432241 | 2.706194326 |
| **CBP** | S2063 | Q92793 | 0.046209337 | 0.953790663 | 1.529325351 |
| **MKP-1** | S359 | P28562 | 0.048462642 | 0.951537358 | 1.736547796 |
| **ROCK2** | S1134/7 | O75116 | 0.050251176 | 0.949748824 | 1.335235318 |

| | | | | | |
|---|---|---|---|---|---|
| **Fyn** | Y420 | P06241 | 0.054586169 | 0.945413831 | 1.496852463 |
| **A-Raf** | Y301 | P10398 | 0.944672698 | 0.055327302 | -2.145914408 |
| **Syk** | Y525/6 | P43405 | 0.94768683 | 0.05231317 | -3.025678652 |
| **HIF2A** | T840 | Q99814 | 0.953227317 | 0.046772683 | -1.71369426 |
| **Rac1** | S71 | P63000 | 0.956010615 | 0.043989385 | -2.176177994 |
| **iNOS** | S909 | P35228 | 0.959586405 | 0.040413595 | -1.581918507 |
| **PLCG1** | Y771 | P19174 | 0.962451241 | 0.037548759 | -1.816040381 |
| **Daxx** | S668/71 | Q9UER7 | 0.965074364 | 0.034925636 | -1.459165917 |
| **IL2RB** | Y364 | P14784 | 0.965617966 | 0.034382034 | -1.948832808 |
| **ERK1** | T202/4 | P27361 | 0.970147937 | 0.029852063 | -1.764253426 |
| **MSK2** | S347 | O75676 | 0.971279178 | 0.028720822 | -1.625341223 |
| **gp130** | Y767 | P40189 | 0.972195063 | 0.027804937 | -1.580191733 |
| **iNOS** | S739 | P35228 | 0.975169646 | 0.024830354 | -1.347776557 |
| **Bad** | S118 | Q92934 | 0.975675385 | 0.024324615 | -1.593990167 |
| **ERK2** | Y205 | P28482 | 0.978745366 | 0.021254634 | -2.109913446 |
| **ERK3** | S189 | Q16659 | 0.979683061 | 0.020316939 | -1.771565013 |
| **RIPK1** | Y384/7/9 | Q13546 | 0.984376253 | 0.015623747 | -1.285943955 |
| **FLT3** | Y597/9 | P36888 | 0.986271203 | 0.013728797 | -1.854424216 |
| **IL-10R-A** | Y496 | Q13651 | 0.987804951 | 0.012195049 | -1.891010914 |
| **PKCT** | T219 | Q04759 | 0.989940275 | 0.010059725 | -1.401619199 |
| **VEGFR3** | Y130/1 | P35916 | 0.990994175 | 0.009005825 | -2.137667104 |
| **IRAK1** | T100 | P51617 | 0.991862373 | 0.008137627 | -1.527571122 |
| **4E-BP1** | T37 | Q13541 | 0.992806839 | 0.007193161 | -2.600597579 |
| **Src** | S96 | P12931 | 0.993747456 | 0.006252544 | -2.356887655 |
| **MSK1** | T581 | O75582 | 0.997733589 | 0.002266411 | -1.912427531 |
| **SOD1** | S98 | P00441 | 0.99799347 | 0.00200653 | -2.440491216 |

## S8. Total Test Proteins in Kinome Array

**Total Kinome Array Test Proteins**

| | | | | |
|---|---|---|---|---|
| 4E-BP1 | CTNNB1 | H-Ras-1 | MEK5 | PPP2CA |
| 4E-BP1 | CTNNB1 | HSP27 | MEKK1 | PTP1B |
| ADCY8 | CTNNB1 | HSP60 | Met | PXN |
| Akt1 | CTSB | HSP70 | Met | Pyk2 |
| Akt1 | CXCR4 | IFNAR1 | MKP-1 | RAC1 |
| Akt1 | cyclin D1 | IFNAR1 | MKP-1 | Raf1 |
| Akt1 | cyclin E1 | IFNGR1 | MKP-1 | Raf1 |
| Akt3 | Cystatin S | IFNGR1 | MLK3 | RasGAP |
| Akt3 | DAPK1 | IGF1R | Mos | Rb |
| APE1 | DAPK1 | IkB-alpha | MSK1 | Rb |
| Aplp1 | DAPK3 | IkB-alpha | MSK2 | RBL2_SYMSP |
| ApoE | DAPK3 | IkB-beta | MSK2 | RelB |
| A-Raf | DAPP1 | IkB-beta | mucin 1 | RhoA |
| ASK1 | Daxx | IKK-alpha | NFAT1 | RIPK1 |
| ASK1 | DNA-PK | IKK-beta | NFAT1 | ROCK2 |
| ASK1 | DNA-PK | IKK-beta | NFAT2 | SEK1 |

| | | | | |
|---|---|---|---|---|
| ATF-2 | Elk-1 | IKK-gamma | NFAT4 | SEK1 |
| ATF-2 | Elk-1 | IKK-gamma | NFκβ-p100 | Shc1 |
| ATF-4 | eNOS | IL-10R-A | NFκβ-p100 | Smad1 |
| axin-1 | EphA1 | IL-16 | NFκβ-p105 | Smad2 |
| Bad | EphA2 | IL1A | NFκβ-p105 | Smad2 |
| BATF | EphA2 | IL2RB | NFκβ-p65 | Smad3 |
| BCAP | EphA2 | IL2RB | NFκβ-p65 | Smad3 |
| BCAP | ERK1 | IL4R | NFκβ-p65 | smMLCK |
| Bcl-2 | ERK2 | IL7R | NGFR | SOD1 |
| Bcl-2 | ERK3 | IL-8R B | Nik | Src |
| Bid | Etk | IL-8R B | Notch 2 | Src |
| BLNK | Ezrin | iNOS | Notch 2 | SRF |
| BLNK | FADD | iNOS | p300 | STAT1 |
| B-Raf | FADD | iNOS | p300 | STAT1 |
| Btk | FAK | IRAK1 | P38 gamma | STAT2 |
| Btk | Fas | IRAK1 | p38-alpha | STAT3 |
| Calmodulin | Fas | IRAK1 | p38-alpha | STAT3 |
| CaMK2-alpha | Fes | IRAK1 | p40phox | STAT4 |
| Casp3 | FGFR1 | IRAK1 | p47phox | STAT4 |
| Casp8 | FGFR1 | IRF-3 | p53 | STAT5B |
| caveolin-1 | FGFR1 | IRF-3 | p53 | STAT5B |
| Cbl | FGFR3 | IRF-3 | p70S6Kb | STAT6 |
| CBP | FGFR3 | IRF-5 | PDGFRb | STMN1 |
| CCR2 | FGFR4 | ITK | PDGFRb | STMN1 |
| CCR5 | FLGE_ECOLI | Jak1 | PIK3R1 | Syk |
| CCR7 | FLT3 | Jak2 | PKACa | TAK1 |
| CCR7 | FLT3 | Jak3 | PKACa | TAK1 |
| CD28 | Fos | JIP1 | PKCA | TBK1 |
| CD45 | FRS2 | JNK1 | PKCA | TNF-R1 |
| CD45 | FRS2 | JNK1 | PKCB | TNFRSF5 |
| Cdc25A | FRS3 | JNK2 | PKCB | TNIK |
| Cdc25A | Fyn | JNK2 | PKCE | TNIK |
| Cdc42 | Fyn | JNK3 | PKCE | TPH1 |
| CDK2 | GCAP2 | Jun | PKCT | TrkB |
| CDK2 | gp130 | Jun | PKCT | TrkC |
| CDK7 | gp130 | Kit | PKG1 | Tyk2 |
| Cot | gp130 | Kit | PKR | VASP |
| CREB | Grb10 | LEF-1 | PKR | VEGFR-1 |
| CREB | Grb2 | LEF-1 | PLCB1 | VEGFR-2 |
| Crk | GSK3-beta | LRRFIP1 | PLCB1 | VEGFR3 |
| CSFR | GSK3-beta | LRRFIP1 | PLCG1 | VEGFR3 |
| CSFR | HIF1A | Lyn | PLCG1 | VIM |
| CSK | HIF2A | MEK1 | PLCG1 | WASP |
| CTLA-4 | HMGA1 | MEK2 | PPARG | XIAP |

S9. Transcription Factor Profiling Array. Transcription factor symbols on top, relative luminocity below.

Adeno-Zhangfei infection – raw data

| AP1 | CDP | GATA | NF-1 | Pit | Stat3 |
|---|---|---|---|---|---|
| AP2 | CREB | GR/PR | NFAT | PPAR | Stat4 |
| AR | E2F-1 | HIF | NF-E2 | PXR | Stat5 |
| ATF2 | EGR | HNF4 | NFkB | Smad SBE | Stat6 |
| Brn-3 | ER | IRF | OCT4 | Sp1 | TCF/LEF |
| C/EBP | Ets | MEF2 | p53 | SRE | TR |
| CAR | FAST-1 | Myb | Pax-5 | STAB1 | YY1 |
| CBF | GAS/ISRE | Myc-Max | Pbx1 | Stat1 | TFIID |
| 1700 | 992 | 1200 | 832 | 1179 | 501 |
| 1128 | 568 | 463 | 471 | 587 | 514 |
| 769 | 916 | 499 | 681 | 416 | 598 |
| 461 | 876 | 626 | 616 | 703 | 758 |
| 1200 | 533 | 649 | 962 | 875 | 745 |
| 466 | 756 | 704 | 595 | 414 | 510 |
| 840 | 804 | 1196 | 684 | 556 | 843 |
| 988 | 954 | 930 | 1240 | 1496 | 1012 |

Adeno-LacZ infection – raw data

| AP1 | CDP | GATA | NF-1 | Pit | Stat3 |
|---|---|---|---|---|---|
| AP2 | CREB | GR/PR | NFAT | PPAR | Stat4 |
| AR | E2F-1 | HIF | NF-E2 | PXR | Stat5 |
| ATF2 | EGR | HNF4 | NFkB | Smad SBE | Stat6 |
| Brn-3 | ER | IRF | OCT4 | Sp1 | TCF/LEF |
| C/EBP | Ets | MEF2 | p53 | SRE | TR |
| CAR | FAST-1 | Myb | Pax-5 | STAB1 | YY1 |
| CBF | GAS/ISRE | Myc-Max | Pbx1 | Stat1 | TFIID |
| 1042 | 571 | 677 | 745 | 668 | 572 |
| 479 | 639 | 465 | 425 | 560 | 460 |
| 573 | 614 | 733 | 534 | 905 | 517 |
| 513 | 761 | 411 | 369 | 489 | 337 |
| 559 | 439 | 556 | 475 | 698 | 410 |
| 796 | 658 | 497 | 550 | 736 | 451 |
| 532 | 645 | 789 | 549 | 721 | 566 |
| 718 | 1047 | 809 | 1040 | 977 | 863 |

## References


1. **Akhova, O., M. Bainbridge, and V. Misra.** 2005. The neuronal host cell factor-binding protein Zhangfei inhibits herpes simplex virus replication. J Virol **79:**14708-18.

2. **Albert, L., M. Karsy, R. Murali, and M. Jhanwar-Uniyal.** 2009. Inhibition of mTOR Activates the MAPK Pathway in Glioblastoma Multiforme. Cancer Genomics Proteomics **6:**255-61.

3. **Alvarez, S., A. Blanco, M. Fresno, and M. A. Munoz-Fernandez.** TNF-alpha contributes to caspase-3 independent apoptosis in neuroblastoma cells: role of NFAT. PLoS One **6:**e16100.

4. **Ameyar, M., M. Wisniewska, and J. B. Weitzman.** 2003. A role for AP-1 in apoptosis: the case for and against. Biochimie **85:**747-52.

5. **Ashkenazi, A., and V. M. Dixit.** 1998. Death receptors: signaling and modulation. Science **281:**1305-8.

6. **Belliveau, D. J., I. Krivko, J. Kohn, C. Lachance, C. Pozniak, D. Rusakov, D. Kaplan, and F. D. Miller.** 1997. NGF and neurotrophin-3 both activate TrkA on sympathetic neurons but differentially regulate survival and neuritogenesis. J Cell Biol **136:**375-88.

7. **Bergmann, A.** 2007. Autophagy and cell death: no longer at odds. Cell **131:**1032-4.

8. **Boone, D. N., Y. Qi, Z. Li, and S. R. Hann.** Egr1 mediates p53-independent c-Myc-induced apoptosis via a noncanonical ARF-dependent transcriptional mechanism. Proc Natl Acad Sci U S A **108:**632-7.

9. **Bortner, C. D., N. B. Oldenburg, and J. A. Cidlowski.** 1995. The role of DNA fragmentation in apoptosis. Trends Cell Biol **5:**21-6.

10. **Boya, P., R. A. Gonzalez-Polo, N. Casares, J. L. Perfettini, P. Dessen, N. Larochette, D. Metivier, D. Meley, S. Souquere, T. Yoshimori, G. Pierron, P. Codogno, and G. Kroemer.** 2005. Inhibition of macroautophagy triggers apoptosis. Mol Cell Biol **25:**1025-40.

11. **Bratton, D. L., V. A. Fadok, D. A. Richter, J. M. Kailey, L. A. Guthrie, and P. M. Henson.** 1997. Appearance of phosphatidylserine on apoptotic cells requires calcium-mediated nonspecific flip-flop and is enhanced by loss of the aminophospholipid translocase. J Biol Chem **272:**26159-65.

12. **Briggs, K. J., I. M. Corcoran-Schwartz, W. Zhang, T. Harcke, W. L. Devereux, S. B. Baylin, C. G. Eberhart, and D. N. Watkins.** 2008. Cooperation between the Hic1 and Ptch1 tumor suppressors in medulloblastoma. Genes Dev **22:**770-85.

13. **Brodeur, G. M.** 2003. Neuroblastoma: biological insights into a clinical enigma. Nat Rev Cancer **3:**203-16.

14. **Brown, T. L., S. Patil, C. D. Cianci, J. S. Morrow, and P. H. Howe.** 1999. Transforming growth factor beta induces caspase 3-independent cleavage of alphaII-spectrin (alpha-fodrin) coincident with apoptosis. J Biol Chem **274:**23256-62.

15. **Brunner, T., C. Wasem, R. Torgler, I. Cima, S. Jakob, and N. Corazza.** 2003. Fas (CD95/Apo-1) ligand regulation in T cell homeostasis, cell-mediated cytotoxicity and immune pathology. Semin Immunol **15:**167-76.

16. **Cannons, J. L., Y. Choi, and T. H. Watts.** 2000. Role of TNF receptor-associated factor 2 and p38 mitogen-activated protein kinase activation during 4-1BB-dependent immune response. J Immunol **165:**6193-204.

17. **Cao, Y., and D. J. Klionsky.** 2007. Physiological functions of Atg6/Beclin 1: a unique autophagy-related protein. Cell Res **17:**839-49.

18. **Castellino, R. C., M. De Bortoli, X. Lu, S. H. Moon, T. A. Nguyen, M. A. Shepard, P. H. Rao, L. A. Donehower, and J. Y. Kim.** 2008. Medulloblastomas overexpress the p53-inactivating oncogene WIP1/PPM1D. J Neurooncol **86:**245-56.

19. **Chen, G., and D. V. Goeddel.** 2002. TNF-R1 signaling: a beautiful pathway. Science **296:**1634-5.

20. **Chinnaiyan, A. M.** 1999. The apoptosome: heart and soul of the cell death machine. Neoplasia **1:**5-15.

21. **Clarke, P. G.** 1990. Developmental cell death: morphological diversity and multiple mechanisms. Anat Embryol (Berl) **181:**195-213.

22. **Cockram, G. P., M. R. Hogan, H. F. Burnett, and R. Lu.** 2006. Identification and characterization of the DNA-binding properties of a Zhangfei homologue in Japanese pufferfish, Takifugu rubripes. Biochem Biophys Res Commun **339:**1238-45.

23. **Cohen, G. M.** 1997. Caspases: the executioners of apoptosis. Biochem J **326 ( Pt 1):**1-16.

24. **Corcelle, E., N. Djerbi, M. Mari, M. Nebout, C. Fiorini, P. Fenichel, P. Hofman, P. Poujeol, and B. Mograbi.** 2007. Control of the autophagy maturation step by the MAPK ERK and p38: lessons from environmental carcinogens. Autophagy **3:**57-9.

25. **Cordenonsi, M., M. Montagner, M. Adorno, L. Zacchigna, G. Martello, A. Mamidi, S. Soligo, S. Dupont, and S. Piccolo.** 2007. Integration of TGF-beta and Ras/MAPK signaling through p53 phosphorylation. Science **315:**840-3.

26. **Crawford, J. R., T. J. MacDonald, and R. J. Packer.** 2007. Medulloblastoma in childhood: new biological advances. Lancet Neurol **6:**1073-85.

27. **Dadakhujaev, S., E. J. Jung, H. S. Noh, Y. S. Hah, C. J. Kim, and D. R. Kim.** 2009. Interplay between autophagy and apoptosis in TrkA-induced cell death. Autophagy **5**.

28. **DeBenedette, M. A., A. Shahinian, T. W. Mak, and T. H. Watts.** 1997. Costimulation of CD28- T lymphocytes by 4-1BB ligand. J Immunol **158:**551-9.

29. **Didenko, V. V., H. Ngo, C. L. Minchew, D. J. Boudreaux, M. A. Widmayer, and D. S. Baskin.** 2002. Caspase-3-dependent and -independent apoptosis in focal brain ischemia. Mol Med **8:**347-52.

30. **Dimitropoulou, A., and J. L. Bixby.** 2000. Regulation of retinal neurite growth by alterations in MAPK/ERK kinase (MEK) activity. Brain Res **858:**205-14.

31. **Edinger, A. L., and C. B. Thompson.** 2004. Death by design: apoptosis, necrosis and autophagy. Curr Opin Cell Biol **16:**663-9.

32. **Elmore, S.** 2007. Apoptosis: a review of programmed cell death. Toxicol Pathol **35:**495-516.

33. **Falcone, S., E. Cocucci, P. Podini, T. Kirchhausen, E. Clementi, and J. Meldolesi.** 2006. Macropinocytosis: regulated coordination of endocytic and exocytic membrane traffic events. J Cell Sci **119:**4758-69.

34. **Feig, C., and M. E. Peter.** 2007. How apoptosis got the immune system in shape. Eur J Immunol **37 Suppl 1:**S61-70.

35. **Fekete, D. M., S. A. Homburger, M. T. Waring, A. E. Riedl, and L. F. Garcia.** 1997. Involvement of programmed cell death in morphogenesis of the vertebrate inner ear. Development **124:**2451-61.

36. **Feng, Z., L. Li, P. Y. Ng, and A. G. Porter.** 2002. Neuronal differentiation and protection from nitric oxide-induced apoptosis require c-Jun-dependent expression of NCAM140. Mol Cell Biol **22:**5357-66.

37. **Fogarty, M. P., B. A. Emmenegger, L. L. Grasfeder, T. G. Oliver, and R. J. Wechsler-Reya.** 2007. Fibroblast growth factor blocks Sonic hedgehog signaling in neuronal precursors and tumor cells. Proc Natl Acad Sci U S A **104:**2973-8.

38. **Frisch, S. M., and H. Francis.** 1994. Disruption of epithelial cell-matrix interactions induces apoptosis. J Cell Biol **124:**619-26.

39. **Fuchs, S. Y., V. Adler, M. R. Pincus, and Z. Ronai.** 1998. MEKK1/JNK signaling stabilizes and activates p53. Proc Natl Acad Sci U S A **95:**10541-6.

40. **Gaur, U., and B. B. Aggarwal.** 2003. Regulation of proliferation, survival and apoptosis by members of the TNF superfamily. Biochem Pharmacol **66:**1403-8.

41. **Gilbertson, R. J., and D. W. Ellison.** 2008. The origins of medulloblastoma subtypes. Annu Rev Pathol **3:**341-65.

42. **Goberdhan, D. C., M. H. Ogmundsdottir, S. Kazi, B. Reynolds, S. M. Visvalingam, C. Wilson, and C. A. Boyd.** 2009. Amino acid sensing and mTOR regulation: inside or out? Biochem Soc Trans **37:**248-52.

43. **Gouzi, J. Y., C. Moog-Lutz, M. Vigny, and N. Brunet-de Carvalho.** 2005. Role of the subcellular localization of ALK tyrosine kinase domain in neuronal differentiation of PC12 cells. J Cell Sci **118:**5811-23.

44. **Gozuacik, D., and A. Kimchi.** 2004. Autophagy as a cell death and tumor suppressor mechanism. Oncogene **23:**2891-906.

45. **Gulati, P., and G. Thomas.** 2007. Nutrient sensing in the mTOR/S6K1 signalling pathway. Biochem Soc Trans **35:**236-8.

46. **Hacker, G.** 2000. The morphology of apoptosis. Cell Tissue Res **301:**5-17.

47. **Han, J., C. Flemington, A. B. Houghton, Z. Gu, G. P. Zambetti, R. J. Lutz, L. Zhu, and T. Chittenden.** 2001. Expression of bbc3, a pro-apoptotic BH3-only gene, is regulated by diverse cell death and survival signals. Proc Natl Acad Sci U S A **98:**11318-23.

48. **Hansen, K., B. Wagner, W. Hamel, M. Schweizer, F. Haag, M. Westphal, and K. Lamszus.** 2007. Autophagic cell death induced by TrkA receptor activation in human glioblastoma cells. J Neurochem **103:**259-75.

49. **Harel, L., B. Costa, M. Tcherpakov, M. Zapatka, A. Oberthuer, L. M. Hansford, M. Vojvodic, Z. Levy, Z. Y. Chen, F. S. Lee, S. Avigad, I. Yaniv, L. Shi, R. Eils, M. Fischer, B. Brors, D. R. Kaplan, and M. Fainzilber.** 2009. CCM2 mediates death signaling by the TrkA receptor tyrosine kinase. Neuron **63:**585-91.

50. **Hengartner, M. O.** 2000. The biochemistry of apoptosis. Nature **407:**770-6.

51. **Henson, P. M., D. L. Bratton, and V. A. Fadok.** 2001. Apoptotic cell removal. Curr Biol **11:**R795-805.

52. **Hogan, M. R., G. P. Cockram, and R. Lu.** 2006. Cooperative interaction of Zhangfei and ATF4 in transactivation of the cyclic AMP response element. FEBS Lett **580:**58-62.

53. **Horvitz, H. R.** 1999. Genetic control of programmed cell death in the nematode Caenorhabditis elegans. Cancer Res **59:**1701s-1706s.

54. **Huang, E. J., and L. F. Reichardt.** 2003. Trk receptors: roles in neuronal signal transduction. Annu Rev Biochem **72:**609-42.

55. **Huynh, M. L., V. A. Fadok, and P. M. Henson.** 2002. Phosphatidylserine-dependent ingestion of apoptotic cells promotes TGF-beta1 secretion and the resolution of inflammation. J Clin Invest **109:**41-50.

56. **Jaeschke, A., M. Karasarides, J. J. Ventura, A. Ehrhardt, C. Zhang, R. A. Flavell, K. M. Shokat, and R. J. Davis.** 2006. JNK2 is a positive regulator of the cJun transcription factor. Mol Cell **23:**899-911.

57. **Julien, J. P., and W. E. Mushynski.** 1998. Neurofilaments in health and disease. Prog Nucleic Acid Res Mol Biol **61:**1-23.

58. **Jung, C. H., S. H. Ro, J. Cao, N. M. Otto, and D. H. Kim.** mTOR regulation of autophagy. FEBS Lett **584:**1287-95.

59. **Jung, E. J., and D. R. Kim.** Control of TrkA-induced cell death by JNK activation and differential expression of TrkA upon DNA damage. Mol Cells **30:**121-5.

60. **Kabeya, Y., N. Mizushima, T. Ueno, A. Yamamoto, T. Kirisako, T. Noda, E. Kominami, Y. Ohsumi, and T. Yoshimori.** 2000. LC3, a mammalian

homologue of yeast Apg8p, is localized in autophagosome membranes after processing. EMBO J **19:**5720-8.

61. **Kanda, H., and M. Miura.** 2004. Regulatory roles of JNK in programmed cell death. J Biochem **136:**1-6.

62. **Kaplan, D. R., and R. M. Stephens.** 1994. Neurotrophin signal transduction by the Trk receptor. J Neurobiol **25:**1404-17.

63. **Kerr, J. F., A. H. Wyllie, and A. R. Currie.** 1972. Apoptosis: a basic biological phenomenon with wide-ranging implications in tissue kinetics. Br J Cancer **26:**239-57.

64. **Kim, J. Y., A. L. Nelson, S. A. Algon, O. Graves, L. M. Sturla, L. C. Goumnerova, D. H. Rowitch, R. A. Segal, and S. L. Pomeroy.** 2003. Medulloblastoma tumorigenesis diverges from cerebellar granule cell differentiation in patched heterozygous mice. Dev Biol **263:**50-66.

65. **Kimmelman, A. C., N. Nunez Rodriguez, and A. M. Chan.** 2002. R-Ras3/M-Ras induces neuronal differentiation of PC12 cells through cell-type-specific activation of the mitogen-activated protein kinase cascade. Mol Cell Biol **22:**5946-61.

66. **Klionsky, D. J., A. M. Cuervo, and P. O. Seglen.** 2007. Methods for monitoring autophagy from yeast to human. Autophagy **3:**181-206.

67. **Kobayashi, Y.** Mechanism underlying silent cleanup of apoptotic cells. Microbiol Immunol **55:**71-5.

68. **Larsen, K. E., and D. Sulzer.** 2002. Autophagy in neurons: a review. Histol Histopathol **17:**897-908.

69. **Lavoie, J. F., L. Lesauteur, J. Kohn, J. Wong, O. Furtoss, C. J. Thiele, F. D. Miller, and D. R. Kaplan.** 2005. TrkA induces apoptosis of neuroblastoma cells and does so via a p53-dependent mechanism. J Biol Chem **280:**29199-207.

70. **Leppa, S., and D. Bohmann.** 1999. Diverse functions of JNK signaling and c-Jun in stress response and apoptosis. Oncogene **18:**6158-62.

71. **Levine, B., and J. Yuan.** 2005. Autophagy in cell death: an innocent convict? J Clin Invest **115:**2679-88.

72. **Li, C., J. I. Macdonald, T. Hryciw, and S. O. Meakin.** Nerve growth factor activation of the TrkA receptor induces cell death, by macropinocytosis, in medulloblastoma Daoy cells. J Neurochem **112:**882-99.

73. **Li, H., L. Liu, D. Xing, and W. R. Chen.** Inhibition of the JNK/Bim pathway by Hsp70 prevents Bax activation in UV-induced apoptosis. FEBS Lett **584:**4672-8.

74. **Lian, J., X. Wu, F. He, D. Karnak, W. Tang, Y. Meng, D. Xiang, M. Ji, T. S. Lawrence, and L. Xu.** A natural BH3 mimetic induces autophagy in apoptosis-resistant prostate cancer via modulating Bcl-2-Beclin1 interaction at endoplasmic reticulum. Cell Death Differ **18:**60-71.

75. **Lodish.** 2004. Molecular Cell Biology, 5th ed. W H Freeman & Co. Pg.: 533-610.

76. **Lowe, S. W., and A. W. Lin.** 2000. Apoptosis in cancer. Carcinogenesis **21:**485-95.

77. **Lu, R., and V. Misra.** 2000. Zhangfei: a second cellular protein interacts with herpes simplex virus accessory factor HCF in a manner similar to Luman and VP16. Nucleic Acids Res **28:**2446-54.

78. **Ludford-Menting, M. J., S. J. Thomas, B. Crimeen, L. J. Harris, B. E. Loveland, M. Bills, S. Ellis, and S. M. Russell.** 2002. A functional interaction between CD46 and DLG4: a role for DLG4 in epithelial polarization. J Biol Chem **277:**4477-84.

79. **Lum, J. J., D. E. Bauer, M. Kong, M. H. Harris, C. Li, T. Lindsten, and C. B. Thompson.** 2005. Growth factor regulation of autophagy and cell survival in the absence of apoptosis. Cell **120:**237-48.

80. **Ma, L., L. Lei, S. R. Eng, E. Turner, and L. F. Parada.** 2003. Brn3a regulation of TrkA/NGF receptor expression in developing sensory neurons. Development **130:**3525-34.

81. **Maiuri, M. C., E. Zalckvar, A. Kimchi, and G. Kroemer.** 2007. Self-eating and self-killing: crosstalk between autophagy and apoptosis. Nat Rev Mol Cell Biol **8:**741-52.

82. **Majno, G., and I. Joris.** 1995. Apoptosis, oncosis, and necrosis. An overview of cell death. Am J Pathol **146:**3-15.

83. **Man, P. S., T. Wells, and D. A. Carter.** 2007. Egr-1-d2EGFP transgenic rats identify transient populations of neurons and glial cells during postnatal brain development. Gene Expr Patterns **7:**872-83.

84. **Marino, G., and C. Lopez-Otin.** 2004. Autophagy: molecular mechanisms, physiological functions and relevance in human pathology. Cell Mol Life Sci **61:**1439-54.

85. **Mark, M. D., Y. Liu, S. T. Wong, T. R. Hinds, and D. R. Storm.** 1995. Stimulation of neurite outgrowth in PC12 cells by EGF and KCl depolarization: a Ca(2+)-independent phenomenon. J Cell Biol **130:**701-10.

86. **Martin, D. N., and E. H. Baehrecke.** 2004. Caspases function in autophagic programmed cell death in Drosophila. Development **131:**275-84.

87. **Matrone, C., R. Marolda, S. Ciafre, M. T. Ciotti, D. Mercanti, and P. Calissano.** 2009. Tyrosine kinase nerve growth factor receptor switches from prosurvival to proapoptotic activity via Abeta-mediated phosphorylation. Proc Natl Acad Sci U S A **106:**11358-63.

88. **Mehler, M. F., P. C. Mabie, D. Zhang, and J. A. Kessler.** 1997. Bone morphogenetic proteins in the nervous system. Trends Neurosci **20:**309-17.

89. **Mercer, J., and A. Helenius.** 2009. Virus entry by macropinocytosis. Nat Cell Biol **11:**510-20.

90. **Ming, L., P. Wang, A. Bank, J. Yu, and L. Zhang.** 2006. PUMA Dissociates Bax and Bcl-X(L) to induce apoptosis in colon cancer cells. J Biol Chem **281:**16034-42.

91. **Misra, V., N. Rapin, O. Akhova, M. Bainbridge, and P. Korchinski.** 2005. Zhangfei is a potent and specific inhibitor of the host cell factor-binding transcription factor Luman. J Biol Chem **280:**15257-66.

92. **Mizushima, N.** 2007. Autophagy: process and function. Genes Dev **21:**2861-73.

93. **Moriyasu, Y., and Y. Ohsumi.** 1996. Autophagy in Tobacco Suspension-Cultured Cells in Response to Sucrose Starvation. Plant Physiol **111:**1233-1241.

94. **Mortimore, G. E., and A. R. Poso.** 1987. Intracellular protein catabolism and its control during nutrient deprivation and supply. Annu Rev Nutr **7:**539-64.

95. **Muragaki, Y., T. T. Chou, D. R. Kaplan, J. Q. Trojanowski, and V. M. Lee.** 1997. Nerve growth factor induces apoptosis in human medulloblastoma cell lines that express TrkA receptors. J Neurosci **17:**530-42.

96. **Nakagawara, A., M. Arima-Nakagawara, N. J. Scavarda, C. G. Azar, A. B. Cantor, and G. M. Brodeur.** 1993. Association between high levels of expression of the TRK gene and favorable outcome in human neuroblastoma. N Engl J Med **328:**847-54.

97. **Nakaya, T., T. Kawai, and T. Suzuki.** 2008. Regulation of FE65 nuclear translocation and function by amyloid beta-protein precursor in osmotically stressed cells. J Biol Chem **283:**19119-31.

98. **Norbury, C. J., and I. D. Hickson.** 2001. Cellular responses to DNA damage. Annu Rev Pharmacol Toxicol **41:**367-401.

99. **Ohta, T., T. Watanabe, Y. Katayama, J. Kurihara, A. Yoshino, H. Nishimoto, and H. Kishimoto.** 2006. TrkA expression is associated with an elevated level of apoptosis in classic medulloblastomas. Neuropathology **26:**170-7.

100. **Okano-Uchida, T., T. Himi, Y. Komiya, and Y. Ishizaki.** 2004. Cerebellar granule cell precursors can differentiate into astroglial cells. Proc Natl Acad Sci U S A **101:**1211-6.

101. **Otter, I., S. Conus, U. Ravn, M. Rager, R. Olivier, L. Monney, D. Fabbro, and C. Borner.** 1998. The binding properties and biological activities of Bcl-2 and Bax in cells exposed to apoptotic stimuli. J Biol Chem **273:**6110-20.

102. **Overmeyer, J. H., A. Kaul, E. E. Johnson, and W. A. Maltese.** 2008. Active ras triggers death in glioblastoma cells through hyperstimulation of macropinocytosis. Mol Cancer Res **6:**965-77.

103. **Park, K. C., K. Shimizu, and T. Hayakawa.** 1998. Interferon yield and MHC antigen expression of human medulloblastoma cells and its suppression during dibutyryl cyclic AMP-induced differentiation: do medulloblastoma cells derive from bipotent neuronal and glial progenitors? Cell Mol Neurobiol **18:**497-507.

104. **Patapoutian, A., and L. F. Reichardt.** 2001. Trk receptors: mediators of neurotrophin action. Curr Opin Neurobiol **11:**272-80.

105. **Patel, T. D., A. Jackman, F. L. Rice, J. Kucera, and W. D. Snider.** 2000. Development of sensory neurons in the absence of NGF/TrkA signaling in vivo. Neuron **25:**345-57.

106. **Pattingre, S., and B. Levine.** 2006. Bcl-2 inhibition of autophagy: a new route to cancer? Cancer Res **66:**2885-8.

107. **Pattingre, S., A. Tassa, X. Qu, R. Garuti, X. H. Liang, N. Mizushima, M. Packer, M. D. Schneider, and B. Levine.** 2005. Bcl-2 antiapoptotic proteins inhibit Beclin 1-dependent autophagy. Cell **122:**927-39.

108. **Peter, M. E., and P. H. Krammer.** 2003. The CD95(APO-1/Fas) DISC and beyond. Cell Death Differ **10:**26-35.

109. **Philippidou, P., G. Valdez, W. Akmentin, W. J. Bowers, H. J. Federoff, and S. Halegoua.** Trk retrograde signaling requires persistent, Pincher-directed endosomes. Proc Natl Acad Sci U S A **108:**852-7.

110. **Porter, A. G., and R. U. Janicke.** 1999. Emerging roles of caspase-3 in apoptosis. Cell Death Differ **6:**99-104.

111. **Qu, X., J. Yu, G. Bhagat, N. Furuya, H. Hibshoosh, A. Troxel, J. Rosen, E. L. Eskelinen, N. Mizushima, Y. Ohsumi, G. Cattoretti, and B. Levine.** 2003. Promotion of tumorigenesis by heterozygous disruption of the beclin 1 autophagy gene. J Clin Invest **112:**1809-20.

112. **Rath, P. C., and B. B. Aggarwal.** 1999. TNF-induced signaling in apoptosis. J Clin Immunol **19:**350-64.

113. **Renehan, A. G., C. Booth, and C. S. Potten.** 2001. What is apoptosis, and why is it important? BMJ **322:**1536-8.

114. **Riccio, A., B. A. Pierchala, C. L. Ciarallo, and D. D. Ginty.** 1997. An NGF-TrkA-mediated retrograde signal to transcription factor CREB in sympathetic neurons. Science **277:**1097-100.

115. **Roberts, D. S., and S. A. Miller.** 1998. Apoptosis in cavitation of middle ear space. Anat Rec **251:**286-9.

116. **Roos, W. P., and B. Kaina.** 2006. DNA damage-induced cell death by apoptosis. Trends Mol Med **12:**440-50.

117. **Rothermundt, M., M. Peters, J. H. Prehn, and V. Arolt.** 2003. S100B in brain damage and neurodegeneration. Microsc Res Tech **60:**614-32.

118. **Rubin, L. L.** 1997. Neuronal cell death: when, why and how. Br Med Bull **53:**617-31.

119. **Russo, A., M. Terrasi, V. Agnese, D. Santini, and V. Bazan.** 2006. Apoptosis: a relevant tool for anticancer therapy. Ann Oncol **17 Suppl 7:**vii115-23.

120. **Sabo, S. L., A. F. Ikin, J. D. Buxbaum, and P. Greengard.** 2003. The amyloid precursor protein and its regulatory protein, FE65, in growth cones and synapses in vitro and in vivo. J Neurosci **23:**5407-15.

121. **Sachs, L. M., B. Abdallah, A. Hassan, G. Levi, A. De Luze, J. C. Reed, and B. A. Demeneix.** 1997. Apoptosis in Xenopus tadpole tail muscles involves Bax-dependent pathways. FASEB J **11:**801-8.

122. **Saelens, X., N. Festjens, L. Vande Walle, M. van Gurp, G. van Loo, and P. Vandenabeele.** 2004. Toxic proteins released from mitochondria in cell death. Oncogene **23:**2861-74.

123. **Savill, J., and V. Fadok.** 2000. Corpse clearance defines the meaning of cell death. Nature **407:**784-8.

124. **Scarlatti, F., C. Bauvy, A. Ventruti, G. Sala, F. Cluzeaud, A. Vandewalle, R. Ghidoni, and P. Codogno.** 2004. Ceramide-mediated macroautophagy involves inhibition of protein kinase B and up-regulation of beclin 1. J Biol Chem **279:**18384-91.

125. **Schneider, P., and J. Tschopp.** 2000. Apoptosis induced by death receptors. Pharm Acta Helv **74:**281-6.

126. **Schweichel, J. U., and H. J. Merker.** 1973. The morphology of various types of cell death in prenatal tissues. Teratology **7:**253-66.

127. **Shaulian, E., and M. Karin.** 2001. AP-1 in cell proliferation and survival. Oncogene **20:**2390-400.

128. **Snider, W. D.** 1994. Functions of the neurotrophins during nervous system development: what the knockouts are teaching us. Cell **77:**627-38.

129. **Sun, Y. L., Y. Zhao, X. Hong, and Z. H. Zhai.** 1999. Cytochrome c release and caspase activation during menadione-induced apoptosis in plants. FEBS Lett **462:**317-21.

130. **Sutherland, C. L., A. W. Heath, S. L. Pelech, P. R. Young, and M. R. Gold.** 1996. Differential activation of the ERK, JNK, and p38 mitogen-activated protein kinases by CD40 and the B cell antigen receptor. J Immunol **157:**3381-90.

131. **Suzuki, K., and Y. Ohsumi.** 2007. Molecular machinery of autophagosome formation in yeast, Saccharomyces cerevisiae. FEBS Lett **581:**2156-61.

132. **Swanson, J. A.** 2008. Shaping cups into phagosomes and macropinosomes. Nat Rev Mol Cell Biol **9:**639-49.

133. **Swanson, J. A., and C. Watts.** 1995. Macropinocytosis. Trends Cell Biol **5:**424-8.

134. **Takeshige, K., M. Baba, S. Tsuboi, T. Noda, and Y. Ohsumi.** 1992. Autophagy in yeast demonstrated with proteinase-deficient mutants and conditions for its induction. J Cell Biol **119:**301-11.

135. **Tamura, K., K. Shimizu, M. Yamada, Y. Okamoto, Y. Matsui, K. C. Park, E. Mabuchi, S. Moriuchi, and H. Mogami.** 1989. Expression of major histocompatibility complex on human medulloblastoma cells with neuronal differentiation. Cancer Res **49:**5380-4.

136. **Thompson, C. B.** 1995. Apoptosis in the pathogenesis and treatment of disease. Science **267:**1456-62.

137. **Trapani, J. A., and M. J. Smyth.** 2002. Functional significance of the perforin/granzyme cell death pathway. Nat Rev Immunol **2:**735-47.

138. **Traverse, S., K. Seedorf, H. Paterson, C. J. Marshall, P. Cohen, and A. Ullrich.** 1994. EGF triggers neuronal differentiation of PC12 cells that overexpress the EGF receptor. Curr Biol **4:**694-701.

139. **Troy, C. M., J. E. Friedman, and W. J. Friedman.** 2002. Mechanisms of p75-mediated death of hippocampal neurons. Role of caspases. J Biol Chem **277:**34295-302.

140. **Trump, B. F., I. K. Berezesky, S. H. Chang, and P. C. Phelps.** 1997. The pathways of cell death: oncosis, apoptosis, and necrosis. Toxicol Pathol **25:**82-8.

141. **Valderrama, X., and V. Misra.** 2008. Novel Brn3a cis-acting sequences mediate transcription of human trkA in neurons. J Neurochem **105:**425-35.

142. **Valderrama, X., N. Rapin, and V. Misra.** 2008. Zhangfei, a novel regulator of the human nerve growth factor receptor, trkA. J Neurovirol **14:**425-36.

143. **Valderrama, X., N. Rapin, V. M. Verge, and V. Misra.** 2009. Zhangfei induces the expression of the nerve growth factor receptor, trkA, in medulloblastoma cells and causes their differentiation or apoptosis. J Neurooncol **91:**7-17.

144. **Vanyushin, B. F., L. E. Bakeeva, V. A. Zamyatnina, and N. I. Aleksandrushkina.** 2004. Apoptosis in plants: specific features of plant apoptotic cells and effect of various factors and agents. Int Rev Cytol **233:**135-79.

145. **Wang, H., J. Li, R. M. Bostock, and D. G. Gilchrist.** 1996. Apoptosis: A Functional Paradigm for Programmed Plant Cell Death Induced by a Host-Selective Phytotoxin and Invoked during Development. Plant Cell **8:**375-391.

146. **Wang, P., J. Yu, and L. Zhang.** 2007. The nuclear function of p53 is required for PUMA-mediated apoptosis induced by DNA damage. Proc Natl Acad Sci U S A **104:**4054-9.

147. **Watson, F. L., H. M. Heerssen, A. Bhattacharyya, L. Klesse, M. Z. Lin, and R. A. Segal.** 2001. Neurotrophins use the Erk5 pathway to mediate a retrograde survival response. Nat Neurosci **4:**981-8.

148. **Wechsler-Reya, R. J., and M. P. Scott.** 1999. Control of neuronal precursor proliferation in the cerebellum by Sonic Hedgehog. Neuron **22:**103-14.

149. **Werneburg, B. G., S. J. Zoog, T. T. Dang, M. R. Kehry, and J. J. Crute.** 2001. Molecular characterization of CD40 signaling intermediates. J Biol Chem **276:**43334-42.

150. **White, K.** 1995. Morphogenesis. Cell death returns to its roots. Curr Biol **5:**371-2.

151. **Wu, Z., P. C. Chang, J. C. Yang, C. Y. Chu, L. Y. Wang, N. T. Chen, A. H. Ma, S. J. Desai, S. H. Lo, C. P. Evans, K. S. Lam, and H. J. Kung.** Autophagy Blockade Sensitizes Prostate Cancer Cells towards Src Family Kinase Inhibitors. Genes Cancer **1:**40-49.

152. **Xu, P., M. Das, J. Reilly, and R. J. Davis.** JNK regulates FoxO-dependent autophagy in neurons. Genes Dev **25:**310-22.

153. **Xue, L., G. C. Fletcher, and A. M. Tolkovsky.** 2001. Mitochondria are selectively eliminated from eukaryotic cells after blockade of caspases during apoptosis. Curr Biol **11:**361-5.

154. **Yang, H., Y. Xia, S. Q. Lu, T. W. Soong, and Z. W. Feng.** 2008. Basic fibroblast growth factor-induced neuronal differentiation of mouse bone marrow stromal cells requires FGFR-1, MAPK/ERK, and transcription factor AP-1. J Biol Chem **283:**5287-95.

155. **Yue, Z., S. Jin, C. Yang, A. J. Levine, and N. Heintz.** 2003. Beclin 1, an autophagy gene essential for early embryonic development, is a haploinsufficient tumor suppressor. Proc Natl Acad Sci U S A **100:**15077-82.

156. **Zaleske, D. J.** 1985. Development of the upper limb. Hand Clin **1:**383-90.

157. **Zeiss, C. J.** 2003. The apoptosis-necrosis continuum: insights from genetically altered mice. Vet Pathol **40:**481-95.

158. **Zhang, J., W. Yan, and X. Chen.** 2006. p53 is required for nerve growth factor-mediated differentiation of PC12 cells via regulation of TrkA levels. Cell Death Differ **13:**2118-28.

159. **Zhang, Y., Y. Wu, Y. Cheng, Z. Zhao, S. Tashiro, S. Onodera, and T. Ikejima.** 2008. Fas-mediated autophagy requires JNK activation in HeLa cells. Biochem Biophys Res Commun **377:**1205-10.